

Coupled modelling of hydrological processes and grassland production in two contrasting climates

^{1*}Nicholas Jarvis, ^{2,3}Jannis Groh, ¹Elisabet Lewan, ¹Katharina H. E. Meurer, ⁴Walter Durka, ⁴Cornelia Baessler⁴, ²Thomas Pütz, ¹Elvin Ruffullayev, ²Harry Vereecken

¹*Soil and Environment, Swedish University of Agricultural Sciences, Uppsala, Sweden*

²*Agrosphere (IBG-3), Institute of Bio- and Geoscience, Forschungszentrum Jülich GmbH, Jülich, Germany*

³*Research Area 1 "Landscape Functioning", Working Group "Hydropedology", Leibniz Centre for Agricultural Landscape Research (ZALF), Müncheberg, Germany*

⁴*Department of Community Ecology (BZF), Helmholtz Centre for Environmental Research (UFZ), Halle, Germany*

*corresponding author (nicholas.jarvis@slu.se)

1 **Abstract**

2 Projections of global climate models suggest that ongoing human-induced climate change will
3 lead to an increase in the frequency of severe droughts in many important agricultural regions
4 of the world. Eco-hydrological models that integrate current understanding of the interacting
5 processes governing soil water balance and plant growth may be useful tools to predict the
6 impacts of climate change on crop production. However, the validation status of these models
7 for making predictions under climate change is still unclear, since few suitable datasets are
8 available for model testing. One promising approach is to test models using data obtained in
9 “space-for-time” substitution experiments, in which samples are transferred among locations
10 with contrasting current climates in order to mimic future climatic conditions. An important
11 advantage of this approach is that the soil type is the same, so that differences in soil
12 properties are not confounded with the influence of climate on water balance and crop
13 growth. In this study, we evaluate the capability of a relatively simple eco-hydrological model
14 to reproduce 6 years (2013-2018) of measurements of soil water contents, water balance
15 components and grass production made in weighing lysimeters located at two sites within the
16 TERENO-SoilCan network in Germany. Three lysimeters are located at an upland site at
17 Rollesbroich with a cool, wet climate, while three others had been moved from Rollesbroich
18 to a warmer and drier climate on the lower Rhine valley floodplain at Selhausen. Four of the
19 most sensitive parameters in the model were treated as uncertain within the framework of
20 the GLUE (Generalized Likelihood Uncertainty Estimation) methodology, while the remaining
21 parameters in the model were set according to site measurements or data in the literature.

22 The model ~~satisfactorily~~satisfactorily accurately reproduced the measurements at both sites, and some
23 significant differences in the posterior ranges of the four uncertain parameters were found.
24 In particular, the results indicated greater stomatal conductance as well an increase in dry
25 matter allocation below-ground and a significantly larger maximum root depth for the three
26 lysimeters that had been moved to Selhausen. As a consequence, the apparent water use
27 efficiency (above-ground harvest divided by evapotranspiration) was significantly smaller at
28 Selhausen than Rollesbroich. Data on species abundance on the lysimeters provide one
29 possible explanation for the differences in the plant traits at the two sites derived from model
30 calibration. These observations showed that the plant community at Selhausen had changed
31 significantly in response to the drier climate, with a significant decrease in the abundance of
32 herbs and an increase in the proportion of grass species. The differences in root depth and
33 leaf conductance may also be a consequence of plasticity or acclimation at the species level.
34 Regardless of the reason, we may conclude that such adaptations introduce significant
35 additional uncertainties into model predictions of water balance and plant growth in response
36 to climate change.

37 1. Introduction

38 Projections of global climate models suggest that ongoing human-induced climate change will
39 lead to an increase in the frequency of severe droughts (Ruane et al., 2018). This may seriously
40 impact production in many important agricultural regions of the world (Tubiello et al., 2007),
41 including managed grasslands (e.g. Kipling et al., 2016; Stanimirova et al., 2019), since key
42 forage species are known to be sensitive to drought (Norris, 1982; Coleman et al., 1989;
43 Silvertown et al., 1994; Jenkinson et al., 1994; Volaire et al., 1998; Meurer et al., 2019).
44 Grasslands are also of major importance in the context of climate change mitigation, since
45 they cover ca. 70% of the global agricultural land area (Foley et al., 2011) and represent a large
46 store of soil organic carbon (SOC) (Li et al., 2018; Bossio et al., 2020). Soil water status affects
47 plant growth through a complex web of direct and indirect mechanisms (Körner, 2015; White
48 et al., 2016; Tardieu et al., 2018; Loka et al., 2019; Gupta et al., 2020). In turn, plant growth,
49 both above- and below-ground, influences the soil water balance through important feedback
50 mechanisms, particularly the regulation of transpiration by leaf area as well as the control of
51 water supply from the soil by root length density and its distribution with depth (Monteith,
52 1986, 1988; Tardieu et al., 2017). Thus, realistic models of the coupled processes of root water
53 uptake, transpiration and plant growth are required to predict reliably the impacts of climate
54 change on the future productive potential of grassland. Eco-hydrological models that attempt
55 to capture these interactions in the soil-plant system are widely used in climate change studies
56 that focus on the prediction of latent and sensible heat fluxes and CO₂ exchange between the
57 land surface and the atmosphere (e.g. Fatichi et al., 2016; Klein et al., 2017; Kellner et al.,
58 2017). Similarly, soil-crop models that integrate current understanding of the interacting
59 processes governing water balance, SOC and nutrient cycling and crop growth (e.g. Robertson
60 et al., 2015; Wu et al., 2016; Stöckle and Kemanian, 2020) are often used as tools to predict
61 the impacts of land use or climate change on crop production and the environment (e.g.
62 Eckersten et al., 2012). These two types of simulation model share many similarities. In the
63 following, we refer to them collectively as SVAT (soil-vegetation-atmosphere [transfer](#)) models.

64 SVAT models employ empirical (or phenomenological) approaches to describe many of the
65 key processes in the soil-plant system. This is especially the case for the processes governing
66 plant growth because the underlying mechanisms are extremely complex and not easily
67 amenable to fundamental descriptions (Boote et al., 2013; Wu et al., 2016). This means that
68 great care is needed in model calibration exercises, given the usual paucity of experimental
69 data in relation to the number of model parameters. In such cases, parameter errors may
70 often compensate for model deficiencies leading to non-unique solutions or 'equifinality'
71 (Beven and Binley, 1992; Beven, 2006). Parameter uncertainty has not always been
72 considered in SVAT model applications (Seidel et al., 2018). Thus, even though a model
73 performs satisfactorily, it may be doing so for the wrong reasons (Kirchner, 2006). As a
74 consequence, model predictions, for example for a future climate, can be seriously in error
75 (Kersebaum et al., 2007, 2015; Bellocchi et al., 2010; He et al., 2017). In this respect, despite
76 their great potential, it is not yet clear how accurately SVAT models can predict the soil water
77 balance and production potential of grasslands in a changing climate because few suitably
78 comprehensive data sets have been available to unequivocally constrain them in model
79 calibration exercises. Several SVAT models specifically designed for grassland agro-ecosystems

80 have been developed (e.g. Joven et al., 2006a,b; [Johnson et al., 2008](#); Jing et al., 2012;
81 Persson et al., 2014). However, with only a few exceptions, previous studies have focused on
82 calibrating these models against data on above-ground biomass production at single sites,
83 with scant focus on hydrological processes and below-ground biomass, and with little
84 attention paid to parameter uncertainty. In a test of the *PaSim* grassland model at the regional
85 scale, Ma et al. (2015) found that although CO₂ and water fluxes between the land surface and
86 atmosphere were reasonably well matched, soil water contents were not accurately simulated
87 during dry periods. Similarly, in a multi-model and multi-site validation exercise, Sándor et al.
88 (2017) noted a variable model performance at sites with contrasting climates. In particular,
89 they demonstrated a failure of the models to simulate correctly root water uptake patterns
90 and biomass production in dry summers and at dry sites. Even though most grassland species
91 are generally comparatively shallow-rooted (Jackson et al., 1996), several previous studies
92 have highlighted the role of sparsely distributed deeper roots in maintaining water uptake,
93 transpiration and growth during droughts (e.g. Kemp and Culvenor, 1994; Volaire et al 1998;
94 Bonos and Murphy, 1999; Zwicke et al., 2015). This suggests that models of root water uptake
95 for grass must account for compensatory mechanisms, whereby water uptake increases from
96 sparsely rooted wetter soil layers to compensate for reductions in water uptake in densely
97 rooted, but dry soil (Jarvis, 2011; Cai et al., 2017).

98 Manipulation experiments have been carried out to simulate the effects of climate change on
99 grasslands in which plant growth has been monitored following controlled alterations in the
100 precipitation regime (e.g. reduced rainfall amount or frequency). However, nearly all of these
101 experiments are of a short-term nature and the treatments imposed have often been extreme
102 and thus not well adapted to climate model projections (e.g. Beier et al., 2012; Hoover et al.,
103 2018). Furthermore, with only a few exceptions (e.g. Bollig and Feller, 2014), drought
104 manipulation experiments have not focused much on the complex interactions between soil
105 hydrological processes, water stress and plant growth, despite their importance. Thus, in most
106 cases, the mechanisms controlling the observed growth responses have not been elucidated
107 in detail, while little data is available from these experiments that could support and test
108 model predictions (Beier et al., 2012; Hoover et al., 2018). An alternative approach is to test
109 model performance against data obtained in “space-for-time” substitution experiments, in
110 which samples are transferred among sites with contrasting current climates in order to
111 approximately mimic likely future climate conditions (Ineson et al., 1998; Pütz et al., 2016).
112 One important advantage of this approach is that the soil type is the same, so that differences
113 in soil properties are not confounded with the influence of climate on soil hydrology and crop
114 growth. Weighing lysimeters are highly suitable study objects in this context, since they enable
115 the measurement of a complete (closed) water balance (Wegehenkel et al., 2008; Heinlein et
116 al., 2017; Groh et al., 2020a). Providing they are sufficiently large in terms of both depth and
117 diameter, weighing lysimeters also represent a relatively natural environment for plant
118 growth as well as allowing the installation of instrumentation to measure soil water status.

119 In this study, we make use of data from the TERENO-SoilCan network, in which large weighing
120 lysimeters containing undisturbed soil monoliths have been transferred among several
121 locations in Germany to emulate expected changes in climate (Zacharias et al., 2011; Pütz et
122 al., 2016; Groh et al., 2020b). ~~Here, in this study, we compare evaluate the capability of a~~

123 ~~relatively simple eco-hydrological model to reproduce~~ six years of measurements of the soil
124 water balance and grassland production ~~made in replicate lysimeters containing the same soil~~
125 ~~type, but located at two different sites with contrasting climates with simulations using a~~
126 ~~simple eco-hydrological model in the Eifel/Lower Rhine Valley observatory (Zacharias et al.,~~
127 ~~2011; Pütz et al., 2016; Bogena et al., 2018).~~ Our main objective with this modelling exercise
128 ~~was to explore and identify some plausible mechanisms that would explain the observed~~
129 ~~responses of the grassland to a change in climate, in terms of biomass production and water~~
130 ~~use efficiency. Three of these lysimeters are located at an upland site at Rollesbroich with a~~
131 ~~cool, wet climate, while three others were moved from Rollesbroich to a warmer, drier climate~~
132 ~~in the Rhine valley at Selhausen.~~

133 2. Materials and methods

134 2.1 Site descriptions, vegetation, soil properties and lysimeter data

135 ~~We make use of measurements made in six undisturbed lysimeters that were sampled at~~
136 ~~Three of these lysimeters are located at an upland site (Rollesbroich) in the Eifel/Lower Rhine~~
137 ~~Valley observatory (Zacharias et al., 2011; Pütz et al., 2016; Bogena et al., 2018). at~~
138 ~~Rollesbroich. Three of these lysimeters were kept at Rollesbroich with a cool, wet climate, while~~
139 ~~the three others were moved from Rollesbroich to a warmer, drier climate in the Rhine valley~~
140 ~~at Selhausen.~~ The station at Rollesbroich (50° 37' N, 6° 18' E) is located on a hilltop site at an
141 elevation of 511 m, while Selhausen (50° 52' N, 6° 27' E) is located on a relatively flat alluvial
142 flood plain in the lower Rhine valley at an altitude of 104 m. The mean annual air temperature
143 at Rollesbroich is 8°C and the mean annual precipitation is 1150 mm. At Selhausen, the mean
144 annual air temperature is 10°C and the mean annual precipitation is 720 mm. A weather
145 station at each site records precipitation, solar radiation, air temperature, air humidity and
146 wind speed at a height of 2 m at a ten-minute time resolution (Pütz et al., 2016), which we
147 aggregated to a daily time step. From these meteorological variables, we calculated daily
148 reference (potential) evapotranspiration for grass with the FAO Penman-Monteith equation
149 (Allen et al., 1998) as a simple comparative measure of the atmospheric demand for water in
150 the two climates. The meteorological data and calculated reference evapotranspiration at the
151 two sites for the period 2013-2018 are shown in the supplementary information (figure S1).

152 The soil at Rollesbroich is a Stagnic Cambisol, with the basic properties shown in Table 1. The
153 soil is a sandy loam in the topsoil, changing abruptly to a clay loam at 24 cm depth. The texture
154 again becomes coarser (sandy loam/loam) in the deep subsoil below 93 cm (Table 1). The
155 original grassland community on the lysimeters extracted at Rollesbroich is classified as a
156 mesic grassland of the Arrhenatheretalia alliance without any clear affiliation to classical plant
157 associations. The community is dominated by *Lolium perenne* L., *Ranunculus repens* L., *Rumex*
158 *acetosa* L., *Taraxacum officinale* L., *Dactylis glomerata* L. and *Trifolium repens* L. During the
159 extraction of the lysimeters at Rollesbroich, grassland roots were observed to extend to ca.
160 40-50 cm depth (J. Groh, T. Pütz, pers. comm.). This is supported by SOC contents measured
161 in the soil profile, which decline abruptly below 50 cm depth (Table 1). The lysimeters are
162 supplied with fertilizer as liquid manure and the vegetation is cut 3 to 4 times per growing
163 season to characterize above-ground biomass production, following the local management

164 practice. During the first four years (2013-2016) of the experimental period, leaf area index
165 was measured on multiple occasions with an LAI-2200C Plant Canopy Analyzer from Licor.
166 Plant height was also measured using a conventional ruler. Plant communities present in the
167 lysimeters were assessed annually during the period 2011 to 2016. Plant species abundance
168 was estimated as the number of grid cells occupied of 64 rectangular cells (10 × 10cm). Based
169 on this data, the relative abundances of three plant functional types (i.e. grasses, legumes and
170 non-legume herbs) were quantified. These observations showed that plant communities
171 changed significantly at both sites, with a general decrease in the abundance of herbs and an
172 increase in the proportion of grass species (figure S2). This change was much less pronounced
173 at Rollesbroich than in the lysimeters transferred to Selhausen, where the plant community
174 composition diverged continuously from the original resident community composition,
175 presumably in response to the move to the warmer and drier climate. The small changes in
176 community composition found at Rollesbroich may be a consequence of the experimental set-
177 up. For example, the lysimeters do not allow for root-ingrowth of rhizomatous herb species.

178 The lysimeters have a surface area of 1 m² and are 1.5 m deep. Weighing devices (load cells)
179 measure weight changes equivalent to a water depth of 0.01 mm. Application of a filter
180 routine to separate signal from noise enables accurate estimations of both precipitation and
181 evapotranspiration from each lysimeter (Peters et al., 2017). Missing precipitation data were
182 filled in a first step using the mean value calculated for all available lysimeters. In a second
183 step, any remaining gaps were then filled using the precipitation measured by the reference
184 precipitation gauge. Water fluxes into and out of the lysimeters at the base are measured and
185 are controlled by continuous measurements of ~~soil-water~~ pressure heads made in the
186 surrounding soil at 1.4 m depth. Soil water contents and pressure heads are measured at a
187 ten-minute time resolution at three depths (10, 30 and 50 cm depth) in the lysimeters using
188 TDR probes and conventional tensiometers (30 and 50 cm depth) or MPS1 matric potential
189 sensors (only at 10 cm depth). A detailed description of the design, construction and
190 extraction of the lysimeters and their installation in the lysimeter stations of the SoilCan
191 network can be found in Pütz et al. (2016). Three lysimeters were moved from Rollesbroich to
192 Selhausen in November 2011. In this study, we make use of measurements made in a six-year
193 period from 2013 to 2018.

194 Table 2 summarizes the annual average water balances measured in the six lysimeters in the
195 six-year period from 2013 to 2018, as well as the average annual harvested biomass and
196 calculations of the water use efficiency, defined as the ratio of harvest to evapotranspiration.
197 In the wet climate at Rollesbroich, actual evapotranspiration was ca. 90% of the potential rate
198 calculated by the FAO version of the Penman-Monteith equation for the period 2013-2018
199 (641 and 710 mm/year respectively), while percolation from the lysimeters was on average
200 42% of the precipitation (442 and 1062 mm/year respectively). Thus, evapotranspiration at
201 Rollesbroich is mostly limited by the available energy and is only rarely limited by water supply
202 (Gebler et al., 2015; Rahmati et al., 2020). Notably, the ratio of actual to potential
203 evapotranspiration was only slightly smaller in the much drier climate of Selhausen than at
204 Rollesbroich (on average 86%, Table 2). Figure 1 shows that a strong limitation of the water
205 supply on evapotranspiration at Selhausen can only be seen in the very dry year of 2018, when
206 the ratio between actual and potential rates fell to ca. 60%. It is also striking that the actual

207 evapotranspiration slightly exceeds precipitation at Selhausen, so that the net percolation at
 208 the base of the lysimeters is negative (i.e. ~~an~~ upwards directed flow; Table 2). This is probably
 209 a result of the topographical position of the site on a low-lying flood plain, such that lateral
 210 groundwater flow from surrounding higher land is sufficient to maintain the supply of water
 211 to the drying plant root zone (i.e. the Selhausen site lies in a discharge area in the landscape).

212 Table 2 shows that the differences in water balance components among the three replicate
 213 lysimeters at both sites are very small. For precipitation, the difference between the largest
 214 and smallest measured totals among the replicates at Rollesbroich and Selhausen is only ca.
 215 3% and 1% of the mean value respectively. Furthermore, the difference in evapotranspiration
 216 between the two lysimeters with the largest and smallest values is equivalent to only 1% of
 217 the precipitation at Selhausen and 2.6% of the precipitation at Rollesbroich. This limited
 218 within-site variation in hydrologic response appears to be consistent with the available data
 219 for soil water contents and pressure heads. The ‘in situ’ water retention data (Figure S3 and
 220 Table S1) suggest that there is limited spatial variation in soil hydraulic properties among the
 221 six lysimeters. Percolation is somewhat more variable (Table 2), despite the fact that the
 222 pressure heads in the surrounding soil at 1.4 m depth controlling water flow at the base of the
 223 lysimeter are also quite similar among the replicates, especially at Rollesbroich (see figure S4).

224 Likewise, harvested biomass at Selhausen was similar in all three replicate lysimeters, whereas
 225 it varied more at Rollesbroich, with one lysimeter clearly an outlier (Ro_Y_013, Table 2). Much
 226 larger nitrate nitrogen concentrations were consistently found at the beginning of the
 227 experiment in the leachate from this lysimeter (Giraud et al. 2021), which suggests that the
 228 larger harvest from Ro_Y_013 may be due to a better nutrient supply from the soil. Table 2
 229 and figure 2 show that the water use efficiency (WUE) of the grassland in the drier climate at
 230 Selhausen was smaller than for the lysimeters at Rollesbroich (Forstner et al., 2021), since
 231 harvests were somewhat smaller and evapotranspiration was larger.

232 In the following, we assess the capability of a relatively simple (parsimonious) eco-hydrological
 233 model to match the data measured in the replicate lysimeters in the two contrasting climates
 234 at Rollesbroich and Selhausen. We also use the model to identify plausible reasons for the
 235 differences in soil hydrology and grassland growth observed between the sites.

236 2.2 Model description

237 2.2.1 Potential evapotranspiration

238 In the longer term, the extent of grass cover can be affected by a changing climate, which will
 239 alter the energy balance partitioning at the land surface. We therefore employ the dual-source
 240 Penman-Monteith equation (Shuttleworth and Wallace, 1985; Shuttleworth and Gurney,
 241 1990), which enables the estimation of potential soil evaporation E_p (m day⁻¹) and potential
 242 transpiration T_p (m day⁻¹) from dynamic plant properties and meteorological variables:

$$243 E_p = \left(\frac{3600 \cdot 24 \cdot C_s}{1000 \cdot \lambda} \right) \frac{c_g}{\lambda} \left[\frac{\Delta R_n + \left\{ \frac{\rho c_p VPD - \Delta r_a^s (R_n - R_{n(s)})}{r_a^a + r_a^s} \right\}}{\Delta + \gamma \left(1 + \left(\frac{r_s^s}{r_a^a + r_a^c} \right) \right)} \right]$$

244 —————(1)

$$T_p = \left(\frac{3600 * 24 * C_c}{1000 * \lambda} \right) \frac{C_p}{\lambda} \left\{ \frac{\Delta R_n + \left(\frac{\rho c_p VPD - \Delta r_a^c R_{n(s)}}{r_a^a + r_a^c} \right)}{\Delta + \gamma \left(1 + \left(\frac{r_s^c}{r_a^a + r_a^c} \right) \right)} \right\} \quad (2)$$

$$C_s = \frac{1}{1 + \left(\frac{R_s R_a}{R_c (R_s + R_a)} \right)} \quad (3)$$

$$C_c = \frac{1}{1 + \left(\frac{R_c R_a}{R_s (R_c + R_a)} \right)} \quad (4)$$

$$R_a = (\Delta + \gamma) r_a^a \quad (5)$$

$$R_c = (\Delta + \gamma) r_a^c + \gamma r_s^c \quad (6)$$

$$R_s = (\Delta + \gamma) r_a^s + \gamma r_s^s \quad (7)$$

where λ is the latent heat of vapourisation (J kg^{-1}), ρ is the air density (kg m^{-3}), C_p is the specific heat of air ($\text{J kg}^{-1} \text{ }^\circ\text{C}^{-1}$), VPD is the vapour pressure deficit (Pa), Δ is the slope of the saturation vapour pressure curve ($\text{Pa } ^\circ\text{C}^{-1}$), γ is the psychrometer constant ($\text{Pa } ^\circ\text{C}^{-1}$), r_s^s is the surface resistance of wet soil (here fixed at 20 s m^{-1}), r_s^c and r_a^c are the bulk unstressed stomatal and boundary layer resistances of the canopy (s m^{-1}), R_n and $R_{n(s)}$ are the net radiation above and below the canopy ($\text{J m}^{-2} \text{ s}^{-1}$) and r_a^s and r_a^a are the aerodynamic resistances from soil to canopy and canopy to the reference height (= 2m) respectively (s m^{-1}), both of which are estimated from wind speed and crop height following the approach described by Shuttleworth and Gurney (1990) and Zhou et al. (2006). Assuming that only half the leaf area contributes to transpiration, the canopy surface resistance r_s^c (s m^{-1}) can be expressed as:

$$r_s^c = \frac{2}{\{k_{sto(max)} f_L f_{t(c)}\} LAI} \quad (8)$$

where $k_{sto(max)}$ is the maximum leaf stomatal conductance (m s^{-1}), LAI is the leaf area index ($\text{m}^2 \text{ m}^{-2}$), $f_{t(c)}$ is a function describing the response of conductance to air temperature (see *Environmental stress functions*) and f_L is a light response function given by:

$$f_L = \left(\frac{R_i}{R_i + R_{50}} \right) \quad (9)$$

where R_i is the incoming radiation ($\text{MJ m}^{-2} \text{ d}^{-1}$) and R_{50} is the half-saturation constant for light (here fixed at $5 \text{ MJ m}^{-2} \text{ d}^{-1}$). The bulk boundary layer resistance r_a^c (m s^{-1}) is given by:

$$r_a^c = \frac{r_b}{LAI} \quad (10)$$

where r_b is the leaf boundary layer resistance (here fixed at 25 s m^{-1}). Radiation interception by the plant canopy is calculated using Beer's law:

$$R_{n(s)} = R_n (1 - f_{int}) \quad (11)$$

$$f_{int} = 1 - e^{-\beta LAI} \quad (12)$$

274 where f_{int} is the fraction of the net radiation intercepted by the plant canopy and β is the
275 extinction coefficient. Net radiation is estimated from incoming solar radiation R_i using the
276 algorithms described in Allen et al. (1998).

277 Rainfall interception is at present not considered in the model. Although interception losses
278 may not be negligible even for a reasonably short grassland plant community (Ataroff and
279 Naranjo, 2009; Hu et al., 2009; Groh et al., 2019), we assume that the errors introduced by
280 ignoring the net increase in evaporation due to rainfall interception will be negligible.

281

282 2.2.2 Water flow, root water uptake and transpiration

283 Some SVAT models use tipping bucket or reservoir models to describe water storage and flow
284 in the soil, even though physical approaches based on Richard's equation are not difficult to
285 parameterize and usually perform better (e.g. Diekkrüger et al., 1995; Kröbel et al., 2010;
286 Guest et al., 2017). Water uptake by plant roots is also represented empirically in many widely
287 used SVAT models (Wang and Smith, 2004; Smithwick et al., 2014). These two issues are to
288 some extent linked, as physics-based models of root water uptake require information on soil
289 water pressures and conductances, while tipping bucket or reservoir models only simulate soil
290 water contents. In principle, water uptake by roots also depends on the 3D architecture of the
291 plant root system as well as the hydraulic properties along multiple flow pathways in the soil
292 and plant (e.g. Raats, 2007). Physics-based models have been developed that can calculate
293 water flow and uptake by a root system explicitly defined in 3D (e.g. Dunbabin et al., 2013;
294 Schnepf et al., 2018). Although some attempts have been made (e.g. Postma et al., 2017;
295 Mboh et al., 2019), these models are not so well suited to coupling to SVAT models due to
296 their high parameter and computational requirements. However, some parsimonious physics-
297 based macroscopic approaches have been developed (e.g. de Jong van Lier et al., 2008, 2013;
298 Couvreur et al., 2012; Javaux et al., 2013; Sulis et al., 2019) that contain no more parameters
299 than the empirical models. The parameters of these models are also easier to estimate since
300 they have a stronger physical basis (de Willigen et al., 2012; Javaux et al., 2013). For the same
301 reason, the predictive use of these models should also be more robust in principle. The
302 simplest physics-based models (e.g. Raats, 2007; de Jong van Lier et al., 2008) only describe
303 flow to the roots and neglect flow and resistances within the plant. In this study, we use the
304 model of root water uptake described by de Jong van Lier (2008), which is coupled with
305 Richards' equation to calculate transient water flow soil water content, θ (m m^{-3}) in a one-
306 dimensional soil profile:

$$307 \quad \frac{d\theta}{dt} = \frac{d}{dz} \left[K(\theta) \left(\frac{d(\psi+z)}{dz} \right) \right] - U \quad (13)$$

308 where t is time (days), z is height (m), K is the soil hydraulic conductivity (m day^{-1}), ψ is the
309 pressure head (m) and U (days^{-1}) is the so-called sink term which accounts for root water
310 uptake. The bottom boundary condition required to solve Richards' equation is specified as
311 the known (measured) pressure head at the base of the simulated soil profile, i.e. at 1.4 m
312 depth. The upper boundary condition to equation 13 is specified as a flux given by the

313 difference between the known precipitation rate and the actual soil evaporation, E_a , which in
 314 turn is given by:

$$315 \quad E_a = \min(q_{max}; E_p) \quad (14)$$

316 where q_{max} is the maximum flow rate towards the soil surface calculated using Darcy's law
 317 from the pressure head in the uppermost soil layer. It can be noted that it was not necessary
 318 to include surface runoff in the model because the soil infiltration capacity was never
 319 exceeded. The soil water retention and hydraulic conductivity functions required to solve
 320 equation 13 are given by the Mualem-van Genuchten model (Mualem, 1976; van Genuchten,
 321 1980), with the matching point hydraulic conductivity, K_{10} (m day⁻¹) set at a pressure head of
 322 -0.1 m (Luckner et al., 1989) and assuming that the residual water content is negligible:

$$323 \quad S = \frac{\theta}{\theta_s} \quad (15)$$

$$324 \quad S = (1 + |\alpha \psi|^n)^{\frac{1}{n}-1} \quad (16)$$

$$325 \quad K(S) = K_{10} \left(\frac{S}{S_{10}}\right)^\tau \left[\frac{1 - \left(1 - S^{\left(\frac{n}{n-1}\right)^{\left(1-\frac{1}{n}\right)}\right)}{1 - \left(1 - S_{10}^{\left(\frac{n}{n-1}\right)^{\left(1-\frac{1}{n}\right)}\right)} \right]^2 \quad (17)$$

326 where S is the degree of saturation (-), S_{10} is the value of S at a pressure head of -0.1 m, θ_s is
 327 the saturated water content (m³ m⁻³), α (m⁻¹) and n (-) are shape parameters and τ is a
 328 parameter that reflects the tortuosity and connectivity of the pore
 329 network/tortuosity/connectivity factor. Equation 13 was solved by explicit finite differences
 330 and Runge-Kutta integration, with the soil profile divided into 25 numerical layers, with
 331 thicknesses varying from 1 cm (the uppermost layer) to 6 cm. A constant time step of 1 minute
 332 was employed to maintain numerical stability. The hydraulic conductivity regulating flow
 333 between two adjacent numerical layers in the soil profile was estimated by arithmetic
 334 averaging.

335 Neglecting water storage changes in the plants, the total water uptake from the root zone
 336 equals the actual transpiration rate, T_a , such that:

$$337 \quad T_a = \sum_i U_i \Delta z_i \quad (18)$$

338 where the subscript i refers to a layer in the root zone and Δz is its thickness. To calculate the
 339 sink term U_i and actual transpiration T_a , we make use of the parsimonious physics-based
 340 model of root water uptake proposed by de Jong van Lier et al. (2008), which implicitly
 341 accounts for compensatory uptake (Jarvis, 2011). Neglecting plant resistances, they derived
 342 the macroscopic water uptake sink term to Richards' equation by upscaling a model of water
 343 flow to a single root based on the concept of matric flux potential M (m² day⁻¹):

$$344 \quad M_i = \int_{\psi_w}^{\psi} K(\psi) d\psi \quad (19)$$

345 where ψ_w is the soil water pressure head at which water uptake by plants ceases. At the
 346 microscopic scale in the soil, M will continuously decrease towards its value at the root/soil

347 interface M_o . In this study, we used the approximate solution derived by de Jong van Lier et
 348 al. (2009) to calculate M for the van Genuchten-Mualem model of soil hydraulic properties.
 349 Assuming that M_o is constant in the root zone and neglecting the effects of root and plant
 350 resistances on flow through the soil-plant system, de Jong van Lier et al. (2008) showed that
 351 the sink term for water uptake by roots in each soil layer can be expressed as:

$$352 \quad U_i = \rho_i (M_i - M_o) \quad (20)$$

353 where ρ is a composite root parameter (m^{-2}) given by (de Jong van Lier, 2008):

$$354 \quad \rho_i = \frac{4}{r_o^2 - a^2 r_{m(i)}^2 + 2(r_o^2 + r_{m(i)}^2) \text{LN}\left(\frac{a r_{m(i)}^2}{r_o^2}\right)} \quad (21)$$

355 where r_o is the root radius, a is the distance to the root (normalized by r_m) at which the soil
 356 water content is equal to the average value in layer i (fixed here at 0.53; de Jong van Lier et
 357 al., 2008) and r_m is the mean half distance to the root surface, which can be calculated from
 358 the effective root length density $R_{LD(i)}$ (m m^{-2}) as:

$$359 \quad r_{m(i)} = \sqrt{\frac{1}{\pi R_{LD(i)}}} \quad (22)$$

360 Actual transpiration is determined by the minimum of the potential transpiration rate, T_p , and
 361 the maximum possible flow rate of water to the root system, T_{max} , which occurs when $M_o=0$
 362 (see equations 18 and 20). Thus, actual transpiration can also be expressed as:

$$363 \quad T_a = \min(T_{max}; T_p) \quad (23)$$

364 where T_{max} is obtained by combining equations 18 and 20 with $M_o=0$:

$$365 \quad T_{max} = \sum_i \rho_i M_i \Delta z_i \quad (24)$$

366 For unstressed plants, $T_{max} \geq T_p$ and $T_a = T_p$. In this case, the unknown value of M_o in equation
 367 20 is calculated by combining equations 18, 20 and 24 and knowing that $T_a = T_p$, which gives:

$$368 \quad M_o = \frac{T_{max} - T_p}{(\sum_i \rho_i \Delta z_i)} \quad ; \quad T_{max} \geq T_p \quad (25)$$

$$369 \quad M_o = 0 \quad ; \quad T_{max} < T_p$$

370 It can be seen from equations 24 and 25 that in any given soil, plant water stress will set in
 371 earlier when potential transpiration rates are high and total root length density is low.

372 2.2.3 Growth model for perennial grassland

373 Even though detailed growth models designed for perennial forage grass are already available
 374 (e.g. Schapendonk et al., 1998; Jing et al., 2012; Persson et al., 2014; Kellner et al., 2017), we
 375 developed a simple generic model for the purpose of this study, which only simulates
 376 vegetative growth. This model is intended to be able to capture the main longer-term
 377 feedback mechanisms between soil water status and grass growth (Tardieu and Parent, 2017)

378 and is designed to be compatible with simpler water uptake models that do not simulate water
 379 potentials, resistances and flows within plants (Manzoni et al., 2013).

380 In the model, net assimilation is calculated using the concept of radiation use efficiency (e.g.
 381 Sinclair and Muchow, 1999), which implicitly assumes a constant ratio of respiration to
 382 photosynthesis (i.e. carbon use efficiency; Gifford, 2003). Furthermore, we assume that
 383 assimilation is limited by light, water and temperature, but not by variations in sub-optimal
 384 plant nutrition. The allocation of assimilates to above- and below-ground biomass depends on
 385 environmental stressors. In this respect, based on empirical knowledge, we assume that water
 386 stress and sub-optimal temperatures will increase the partitioning of assimilates to roots (e.g.
 387 Jones et al., 1980a; Kahmen et al., 2005; Hui and Jackson, 2006; Wedderburn et al., 2010;
 388 Skinner and Comas, 2010; Padilla et al., 2013; Nosalewicz et al., 2018; Meurer et al., 2019).
 389 Excess carbohydrates produced by grasses during periods of “sink-limited” growth are stored
 390 as non-structural reserves, mostly in the tiller bases and roots (Thomas, 1991; Johansson,
 391 1993; Volaire et al., 1998; Thomas and James, 1999; Østrem et al., 2011; Martínez-Vilalta et
 392 al., 2016; Hofer et al., 2017; Katata et al., 2020). These non-structural carbohydrates
 393 contribute to rapid recovery of growth after drought or defoliation by grazing or harvesting
 394 (Morvan-Bertrand et al., 1999; Jing et al., 2012; Schmitt et al., 2013; Benot et al., 2019).
 395 However, for the sake of simplicity, our growth model only tracks total biomasses in above-
 396 and below-ground compartments and does not explicitly account for reserves of non-
 397 structural carbohydrates.

398 The loss of both above- and below-ground biomass by diverse mechanisms (e.g. herbivory,
 399 exudation, root decay) is modelled in a simple way as a lumped first-order process. Although
 400 root longevity can be affected by drought (e.g. Chen and Brassard, 2013), this is neglected in
 401 the model for reasons of simplicity. Root systems also show plastic responses to
 402 environmental conditions, such that growth of new roots takes place where water is easily
 403 available, while root dieback occurs in dry soil (e.g. Jupp and Newman, 1987; DaCosta et al.,
 404 2004; Wedderburn et al., 2010). Dynamic modeling of root proliferation and loss in response
 405 to soil conditions remains a very difficult task (e.g. Wang and Smith, 2004; Boote et al., 2013;
 406 Smithwick et al., 2014; Stöckle and Kemanian, 2020). Here, for the sake of simplicity, we
 407 assume that the distribution of root biomass and length within the root zone are constant, as
 408 well as the maximum depth of roots in the profile. With these assumptions, changes in the
 409 below-ground (root) biomass in any soil layer i , $B_{bg(i)}$ (kg dry matter m^{-2}) are given by:

$$410 \quad \frac{dB_{bg(i)}}{dt} = f_{bg} A f_{r(i)} - k_{bg} B_{bg(i)} \quad (26)$$

411 where k_{bg} is a first-order rate constant for root biomass loss (d^{-1}), A ($kg\ m^{-2}\ d^{-1}$) is the dry matter
 412 assimilation rate, f_{bg} is the fraction of dry matter production partitioned to roots and $f_{r(i)}$ is the
 413 fraction of this root production allocated to layer i , which is prescribed by a logistic dose
 414 response function (Schenk and Jackson, 2002; Fan et al., 2016; Metselaar et al., 2019):

$$415 \quad f_{r(i)} = \left[\frac{1}{1 + \left(\frac{D_U}{D_{50}}\right)^c} \right] - \left[\frac{1}{1 + \left(\frac{\min(D_L; D_r)}{D_{50}}\right)^c} \right] ; \quad D_r > D_U \quad (27)$$

416 $f_{r(i)} = 0$; $D_r \leq D_U$

417 where c is a shape factor, D_U and D_L are the depths to the upper and lower boundaries of layer
 418 i , D_r is an effective root depth, which we define as the depth above which 95% of the roots are
 419 located and D_{50} is the depth above which 50% of the root biomass is found, such that:

420
$$D_{50} = \frac{D_r}{\left(\frac{1}{0.95} - 1\right)^{\frac{1}{c}}} \quad (28)$$

421 With this approach, 5% of the roots are located below the maximum root depth. In the model,
 422 we distribute this extra root biomass to the uppermost two numerical layers in equal amounts.

423 The assimilation rate A in equation 26 is calculated as a function of incoming solar radiation
 424 R_s ($\text{MJ m}^{-2} \text{ day}^{-1}$) and two dimensionless stress functions, $f_{t(p)}$ and $f_{w(p)}$ varying between zero
 425 and unity to represent the effects of temperature and water stress on dry matter production:

426
$$A = f_{int} R_s RUE_{max} f_{t(p)} f_{w(p)} \quad (29)$$

427 where RUE_{max} is the maximum radiation use efficiency (kg MJ^{-1}). The root allocation fraction
 428 f_{bg} in equation 26 is calculated as a function of plant stressors (i.e. air temperature, water
 429 stress) and “sink strength”, represented here by the fraction of radiation intercepted, f_{int} , using
 430 an approach based on the simple model concept outlined by Friedlingstein et al. (1999):

431
$$f_{bg} = f_{bg(opt)} \left(\frac{2 f_{int}}{f_{int} + \min(f_{t(a)}; f_{w(a)})} \right) \quad (30)$$

432 where $f_{bg(opt)}$ is the fraction of assimilates partitioned below-ground when the conditions for
 433 above-ground production are optimal (i.e. full canopy, optimal temperature and no water
 434 stress) and $f_{t(a)}$ and $f_{w(a)}$ are response functions to account for the effects of sub-optimal
 435 conditions of temperature and water on allocation. With this approach, sub-optimal
 436 environmental conditions (extreme air temperatures, plant water stress) increase the
 437 proportion of assimilates partitioned to roots, whereas a loss of leaf area (e.g. due to harvest)
 438 triggers an increased allocation of assimilates to the above-ground biomass (see figure S5).

439 Changes in above-ground biomass, B_{ag} (kg m^{-2}) are given by:

440
$$\frac{dB_{ag}}{dt} = (1 - f_{bg})A - k_{ag} \max(1 - f_{t(a)}; 1 - f_{w(a)}) B_{ag} - \Gamma \left(1 - \frac{H_{cut}}{H}\right) \left(\frac{B_{ag}}{\Delta t}\right) \quad (31)$$

441 where Γ is a binary variable, indicating the occurrence of harvest of above-ground biomass
 442 (zero for no harvest, 1 for harvest), H_{cut} is the cutting height at harvest (here set to 0.01 m), H
 443 is the grass height at harvest (m), Δt is the time step in the model and k_{ag} is a rate coefficient
 444 (d^{-1}) regulating the loss of above-ground biomass by senescence and leaf fall, which is also
 445 promoted by sub-optimal temperatures or plant water stress, employing the same empirical
 446 functions used for assimilate partitioning between above-and below-ground biomass. In this
 447 model, we do not account for standing dead above-ground biomass, which would alter the
 448 partitioning of solar radiation between soil and plant, without contributing to transpiration
 449 and assimilation, since we assume that the loss of green leaf area results in immediate litter-
 450 fall. However, it would be straightforward to incorporate standing dead biomass in future
 451 versions of the model, for example in the way described by Montaldo et al. (2005).

452 Feedbacks from the plant growth model to the hydrological model are provided by the leaf
 453 area index, LAI, and effective root length density, $R_{LD(i)}$, which are calculated as:

$$454 \quad LAI = B_{ag} S_{leaf} \quad (32)$$

$$455 \quad R_{LD(i)} = \varepsilon \left(\frac{B_{bg(i)}}{z_i} \right) S_{root} \quad (33)$$

456 where S_{leaf} ($m^2 \text{ kg}^{-1}$) and S_{root} ($m \text{ kg}^{-1}$) are the specific leaf area and specific root length and ε is
 457 the fraction of the total root length that is effective for water uptake (Faria et al., 2010). The
 458 root length density affects the soil resistance to water uptake by roots (equations 21 and 22),
 459 while the leaf area index affects both canopy and aerodynamic resistances (equations 8 and
 460 10) as well as the interception of radiation by the canopy (equation 12). -The height of the
 461 crop also acts as a feedback control on the water balance, since it affects the aerodynamic
 462 resistances to evapotranspiration (equations 1 to 7). The height of the grass cover is not
 463 explicitly simulated in our relatively simple growth model. Instead, we calculate plant height
 464 as a function of simulated LAI, based on the data from both sites (see figure S6).

465 2.2.4 Environmental stress functions

466 As in other models of crop growth (Wu et al., 2016), we use the ratio of actual to potential
 467 transpiration to represent the effects of water stress on assimilation via stomatal closure:

$$468 \quad f_{w(p)} = \frac{T_a}{T_p} \quad (34)$$

469 Water stress also limits crop growth without affecting photosynthesis by several different
 470 mechanisms (Körner, 2015; White et al., 2016; Tardieu et al., 2018; Loka et al., 2019; Gupta et
 471 al., 2020). Many crop models calculate limitations on leaf growth as a threshold function of
 472 the soil water deficit in the root zone. Here, we make use of the matric flux potential at the
 473 root surface M_o (see equations 20 and 25) as a measure of plant water stress, since it should
 474 be more physically and physiologically meaningful. We therefore define a second water stress
 475 index as a threshold response function of M_o , varying between zero and unity, which regulates
 476 dry matter allocation and leaf loss in the model (equations 30 and 31):

$$477 \quad f_{w(a)} = 1 \quad ; \quad M_o \geq M_{o(crit)} \quad (35)$$

$$478 \quad f_{w(a)} = \frac{M_o}{M_{o(crit)}} \quad ; \quad M_o < M_{o(crit)}$$

479 where $M_{o(crit)}$ is a critical value of M_o , which is in turn calculated from a user-defined value of
 480 a critical pressure head at the soil/root interface, $\psi_{o(crit)}$.

481 As in many soil-crop models (Wu et al., 2016), the temperature response function in equations
 482 8 and 29 to 31 is modelled with a piece-wise linear function (figure S7):

$$483 \quad f_{t(c,p,a)} = 0 \quad ; \quad T < T_b \text{ or } T > T_c \quad (36)$$

$$484 \quad f_{t(c,p,a)} = \left(\frac{T - T_b}{T_{o(low)} - T_b} \right) \quad ; \quad T_b \leq T \leq T_{o(low)}$$

485 $f_{t(c,p,a)} = \left(\frac{T_c - T}{T_c - T_{o(high)}} \right)$; $T_{o(high)} \leq T \leq T_c$

486 $f_{t(c,p,a)} = 1$; $T \geq T_{o(low)}$ and $T \leq T_{o(high)}$

487 where T is the mean air temperature (°C), $T_{o(low)}$ and $T_{o(high)}$ define the optimum temperature
 488 (°C) range at which $f_{t(p,a)}$ equals unity and T_b and T_c are the base and ceiling temperatures (°C)
 489 at which the function equals zero. Different values for the parameters in equation 36 can be
 490 assigned for transpiration ($f_{t(c)}$), assimilation ($f_{t(p)}$) and allocation and leaf fall ($f_{t(a)}$).

491

492

493

494 **2.3 Model application**

495 2.3.1 Modelling strategy

496 In this study, uncertainty in the model parameterization has been addressed through Monte
 497 Carlo simulations following the GLUE methodology (see *Sensitivity and uncertainty analysis*).
 498 In principle, it would be possible to apply the model individually to each lysimeter in such an
 499 approach. However, this would have been far too demanding of computer resources. Instead,
 500 recognizing the comparatively small differences in hydrological behavior among the three
 501 replicates at each site (Table 1) and the fact that the same soil type is present at both sites,
 502 we decided to simplify the analysis by assuming a common parameterization for the soil
 503 hydraulic properties in ~~the replicate all six~~ lysimeters at each site. Similarly, we also neglected
 504 the small differences in boundary conditions among the replicate lysimeters at each site. Thus,
 505 precipitation (Table 1; figure S1) and pressure heads at the bottom boundary (figure S4)
 506 measured for one lysimeter at each site (Ro_Y_015 at Rollesbroich and Se_Y_026 at
 507 Selhausen) were used to represent all three replicates. This approach also implicitly assumes
 508 that we can neglect the likelihood of small differences in initial conditions among the
 509 replicates at each site. Initial soil water pressure head profiles at each site were set according
 510 to the results of preliminary simulations involving “trial and error” calibration to measured
 511 early time water outflows from the lysimeters. Initial above- and below-ground plant
 512 biomasses were calculated assuming that the roots constituted 80% of the total biomass and
 513 that the initial leaf area index was 1.5. It can be noted that model predictions quickly become
 514 independent of these initial guesses.

515 2.3.2 Soil hydraulic parameters

516 Four horizons were identified from a soil profile description at the Rollesbroich site (Table 1).
 517 Common parameters of the Mualem-van Genuchten model were estimated for each horizon
 518 from a combination of direct measurements and pedotransfer functions (Table 3). The paired
 519 TDR and tensiometer measurements obtained in the lysimeters at 30 and 50 cm depth were
 520 utilized to estimate common water retention parameters at the two sites for the horizons at
 521 24-48 and 48-90 cm depth by least-squares fitting (Table 3 and figure S3). We used the HYPRES
 522 class pedotransfer functions (Wösten et al., 1999) to estimate the van Genuchten water

523 retention parameters from the soil textural class in the deep subsoil (90-140 cm depth) where
524 no data was available. The measurements from the matric potential sensors installed in the
525 uppermost soil horizon (0-24 cm depth) appeared to be unreliable. We therefore also used
526 the HYPRES pedotransfer functions to estimate the shape parameter n in the topsoil, while α
527 was set equal to the same value as the deeper horizons. Saturated water contents clearly
528 differed between the two sites in the uppermost horizon and were estimated from the data
529 by eye. The reasons for this are not clear. With only three replicates, it could be a result of
530 chance spatial variation. However, at least two physical explanations appear plausible. It is
531 possible that more optimal soil moisture conditions at Selhausen have led to faster
532 mineralization rates of soil organic matter, leading to a decline in the organic matter content
533 and a concomitant increase in soil bulk density (i.e. a loss of porosity, Meurer et al., 2020). It
534 may also be the case that the drier soil surface conditions at Selhausen have reduced soil
535 wettability (Robinson et al., 2019). Hydraulic conductivity at a pressure head of -10 cm (see
536 table 3) was estimated from clay content in each horizon using the pedotransfer function
537 developed by Jarvis et al. (2013).

538 2.3.3 Sensitivity and uncertainty analysis

539 A comprehensive uncertainty analysis treating a large number of model parameters as
540 uncertain was not feasible in this study from the point of view of both data support and
541 computational capacity, even for the comparatively parsimonious model used in this study.
542 We therefore performed a preliminary Monte Carlo sensitivity analysis to support the
543 selection of a limited number of parameters to include in the uncertainty analysis. We ran 500
544 simulations for each site for the period 2013-2018 with parameter values obtained by Latin
545 hypercube sampling from uniform distributions (table S2 in the supplementary information).
546 We quantified the sensitivity of two target outputs (i.e. total evapotranspiration and harvest
547 during the experimental period) to model parameters using Spearman rank partial correlation
548 coefficients. The sampled ranges for the plant parameters in the model were selected to
549 reflect variations based on information in the literature. Three soil hydraulic parameters were
550 also included in this analysis (K_{10} , α and n). This was done by applying scaling factors (see table
551 S2) to the parameter values in Table 3 to broadly reflect the uncertainty arising from the use
552 of pedotransfer functions as well as the spatial variations in the water retention curves derived
553 from the lysimeter measurements (figure S3). It should be noted here that the resulting ranges
554 adopted for the two van Genuchten parameters encompass the differences found among the
555 six lysimeters at both depths. Table S2 shows the results. In general, evapotranspiration and
556 harvest is much more sensitive to many of the plant parameters than to variation in the soil
557 hydraulic properties, which lends support to a modelling strategy in which soil hydraulic
558 properties are set to identical values for all lysimeters. We therefore focused the uncertainty
559 analysis on investigating differences in key plant parameters between the two sites.

560 Of the many highly sensitive plant parameters (Table S2), we decided to treat four as
561 uncertain: the radiation extinction coefficient β , the maximum stomatal conductance $k_{sto(max)}$,
562 the maximum root depth D_r and the limiting pressure head $\psi_{o(crit)}$ that controls dry matter
563 (DM) allocation between above- and below-ground compartments as well as the rate of leaf
564 loss. Several subjective criteria underpin this selection. Firstly, they are among the most highly

565 sensitive parameters for both evapotranspiration and harvest yields (Table S2). In this respect,
 566 with the exception of $T_{o(low)}$, it seems that plant parameters controlling temperature response
 567 are much less sensitive than those regulating water stress (Table S2). Secondly, in addition to
 568 the changes in plant community composition, there are also some known mechanisms of plant
 569 acclimation (e.g. Vincent et al., 2020) that could explain why these four parameters might
 570 plausibly take different values at the two sites. Finally, the effects on these four model
 571 parameters on the model outputs are unlikely to be strongly correlated with one another. This
 572 would not be the case for some of the other sensitive parameters. For example, the radiation
 573 extinction coefficient β would be correlated with the maximum radiation use efficiency, while
 574 $\psi_{o(crit)}$ would be correlated with both the parameter controlling DM allocation under optimal
 575 conditions, $f_{bg(opt)}$, as well as the effective root fraction, ε . The remaining plant parameters in
 576 the model were therefore set to fixed values estimated from data in the literature (Table 4),
 577 prioritizing field studies rather than pot experiments, as the development of drought and the
 578 plant response to stress are known to be strongly affected by restricted root zones (Jones et
 579 al., 1980a,b). Specific leaf area was set to $142 \text{ cm}^2 \text{ g}^{-1}$ based on the measurements of above-
 580 ground biomass and leaf area index for the combined dataset at both sites (see figure S6). The
 581 relationship shown in figure S6 shows some scatter, but no systematic difference between the
 582 sites is apparent. In this respect, Norris (1982) also found no significant differences in specific
 583 leaf area for *Lolium perenne* in droughted, control and irrigated plots.

584 We used the GLUE (Generalized Likelihood Uncertainty Estimation; Beven and Binley, 1992;
 585 Beven 2006) methodology to account for parameter uncertainty. The objective of this
 586 informal Bayesian approach is not to find a single optimum parameter set by calibration, as it
 587 acknowledges that many different parameterizations will perform equally well (so-called
 588 “equifinality”), not least as a consequence of the inevitability of model (structural) error. The
 589 objective of GLUE is therefore to identify acceptable (“behavioural”) parameterizations. To
 590 support this analysis, we ran 2000 simulations for each site, with parameter sets determined
 591 using Latin Hypercube sampling from the prior uncertainty ranges for the four uncertain
 592 parameters shown in Table 5. GLUE involves several subjective decisions, two of the most
 593 important ones being the choice of a likelihood function (i.e. a measure of goodness-of-fit)
 594 and deciding on the criteria that should be used to determine whether a simulation is
 595 acceptable or not. We considered that a parameterization was acceptable if two criteria were
 596 satisfied. The first uses calculations of the model efficiency, ME , for the six observed time
 597 series of data (i.e. water contents at three depths, evapotranspiration rates, LAI, harvests):

$$598 \quad ME = \frac{\sum_{i=1}^m (O_i - \bar{O})^2 - \sum_{i=1}^m (O_i - P_i)^2}{\sum_{i=1}^m (O_i - \bar{O})^2} \quad (37)$$

599 where O and P are the observed and simulated values for a given data type and m is the
 600 number of observations. The maximum value of ME is one, when predictions and observations
 601 are identical, while a negative value implies a poor model, since it means that taking the
 602 average of the observations would give a better prediction. A simulation was considered
 603 acceptable if i.) the model efficiency for all six data types was within 0.5 of the maximum value
 604 for that data series, and ii.) both the simulated annual average evapotranspiration AET
 605 (mm/year) and overall (apparent) water use efficiency WUE (kg DM m^{-3}) were within
 606 acceptable limits roughly defined by the observations (see Table 2):

607 *At Rollesbroich: $610 < AET < 660$ and $1.0 < WUE < 1.2$*

608 *At Selhausen: $680 < AET < 730$ and $0.85 < WUE < 1.05$*

609 This second criterion ensures that the acceptable parameterizations respect the overall broad
610 differences observed in the water balance components and harvest yields between the two
611 sites. Note that the acceptable limit for WUE at Rollesbroich makes no attempt to “honour”
612 the data from lysimeter Ro_Y_013, since it is considered an outlier, as discussed earlier. In
613 total, 35 simulations at Rollesbroich and 57 at Selhausen satisfied these criteria. It is desirable
614 to have the same number of acceptable parameter sets at each site. From these acceptable
615 simulations, we therefore selected the 30 best simulations at each site (i.e. 1.5% of the total
616 number of simulations) according to the average model efficiency for the six data types.

617

618 **3. Results and discussion**

619 **3.1 Acceptable parameter values**

620 The distributions of the acceptable values for the four uncertain parameters are shown in
621 figure 3, while posterior parameter ranges defined by different percentiles of these
622 distributions are presented in table 5. The posterior uncertainty ranges are much smaller than
623 the prior uncertainty ranges, which suggests that values for all four uncertain parameters
624 were clearly identifiable from the data. No differences between the two sites were found for
625 two of the parameters, the radiation extinction coefficient β and $\psi_{o(crit)}$ the parameter
626 controlling dry matter allocation and leaf loss as a function of water stress ($p = 0.98$ and 0.16
627 respectively). The derived values of $\psi_{o(crit)}$ (median value of -271 cm at both sites, Table 5) are
628 much larger than ψ_w ($= -150$ m, Table 4), which indicates that water stress affects above-
629 ground plant growth long before stomatal closure limits transpiration and assimilation
630 (Staniak and Kocoń 2015; Körner, 2015; Loka et al., 2019). This has been shown experimentally
631 for droughted field-grown grass/clover pastures by Jones et al. (1980a,b) and Hofer et al.
632 (2017). The values of the radiation extinction coefficient (inter-quartile range = $0.51-0.65$ at
633 both sites) are typical of values reported for grassland ecosystems (Zhang et al., 2014).

634 In contrast, the results of the GLUE analysis suggest that both the maximum root depth and
635 the unstressed stomatal conductance have increased significantly for the lysimeters moved to
636 Selhausen ($p < 0.0001$ for both). The estimated root depth at Rollesbroich (ca. 56 cm) matches
637 observations made at the site at the time of extraction of the lysimeters reasonably well. The
638 simulations suggest that the maximum root depth at Selhausen has increased to ca. 80 cm,
639 while the maximum stomatal conductance has roughly doubled. The mechanisms underlying
640 these changes are not clear. One reason may be the significant changes observed in the plant
641 community composition at Selhausen compared with the original resident plant community
642 (figure S2), as plant traits may differ significantly between herbs and grasses. Another likely
643 reason is that one or more of the dominant species adapted to the new climate. In this respect,
644 plants are known to acclimatize to environmental stresses ~~at a range of time scales~~ by various
645 physiological and morphological mechanisms ~~-(e.g. Maseda and Fernández, 2006; Nicotra et~~
646 ~~al., 2010; Nicotra and Davidson, 2010; Manzoni et al., 2013; Bartlett et al., 2014; Tardieu et~~

647 al., 2018; Vincent et al., 2020). For example, it is known that many plant species, including
648 perennial ryegrass (Wedderburn et al., 2010), may respond to drought by developing deeper
649 root systems. Although the mechanisms are still imperfectly understood, recent research
650 suggests that various alterations in leaf physiology induced by heat stress may increase leaf
651 hydraulic conductance, thereby enhancing transpiration rates and the degree of evaporative
652 cooling (Sadok et al., 2021).

653 3.2 Soil hydrology

654 Figures 4 and 5 show comparisons of the acceptable simulations at the two sites with the soil
655 water contents measured at the three depths in the lysimeters and daily evapotranspiration
656 rates respectively. The model efficiencies for these simulations are shown in table 6. Figure S8
657 shows measured and simulated values of accumulated evapotranspiration. Figure 6 compares
658 measured annual average evapotranspiration and percolation in the period 2013-2018 with
659 the simulations. ~~Taken together, these results show that the model performs very well,~~
660 ~~matching the temporal dynamics in the high-time resolution data on state variables and fluxes~~
661 ~~as well as reproducing the differences in the overall water balances at the two sites. This is~~
662 ~~probably because the macroscopic sink term describing root water uptake that we coupled to~~
663 ~~Richards' equation has a reasonably strong physical basis. In particular, this model implicitly~~
664 ~~accounts for the mechanism of "compensatory" root water uptake, something which is clearly~~
665 ~~necessary in order to reproduce the extensive drying in the root zone observed in the~~
666 ~~Selhausen lysimeters, with very little reduction in water uptake and transpiration.~~

667 Figure 7 shows some terms of the simulated water balances that were not measured. Potential
668 evapotranspiration calculated ~~internally~~ in the model by the Shuttleworth-Wallace version of
669 the Penman-Monteith equation as a dynamic function of leaf area development at the two
670 sites is very similar to the estimates obtained by the FAO version (Figure 7; table 2), which
671 only treats the vegetation implicitly. This is in spite of the fact that the balance between
672 simulated soil evaporation and transpiration differs strongly between the two sites, with soil
673 evaporation being a much larger component of the water balance at Rollesbroich (Figure 7),
674 where it comprises ca. 70% of the total evapotranspiration. There may be several reasons why
675 soil evaporation is such an important term in the water balance at Rollesbroich, including the
676 wet climate with high wind speeds (Groh et al., 2019) ~~the capillary nature of the soil~~ and ~~also~~
677 the fact that the grassland is harvested 3-4 times during the growing season, which exposes
678 the soil surface to evaporation. In contrast, soil evaporation is much smaller (ca. 50% of total
679 evapotranspiration) in the drier climate at Selhausen, despite greater incoming radiation,
680 presumably because drying of the soil surface in summer frequently reduced evaporation
681 below the potential rate (figure 7).

682 Figure 7 shows that the model simulates only small reductions of transpiration due to water
683 stress and stomatal closure at both sites ($T_a < T_p$), which matches the inference derived from
684 comparing the lysimeter data with the FAO estimates of potential evaporation (figure 1). This
685 result is not especially surprising for the grassland growing in the wet climate at Rollesbroich,
686 but the inference of very limited reductions in water uptake and transpiration in the Selhausen
687 lysimeters despite the extensive drying observed in the root zone (figure 5), ~~it~~ does require
688 further analysis and explanation ~~for the much drier Selhausen site.~~ The macroscopic sink term

689 describing root water uptake that we coupled to Richards' equation implicitly accounts for
690 "compensatory" root water uptake (Jarvis, 2011). Our results suggest these that
691 compensation mechanisms are extremely efficient at the Selhausen site. Figure 8 shows the
692 simulated time-courses of the two water stress functions in the model. Short periods of
693 stomatal closure induced by water stress occur every summer at Selhausen in most of the
694 acceptable model simulations, with one more extended period of drought stress (ca. 1 to 2
695 weeks) in 2018. However, overall, the extent and severity of reductions in transpiration due
696 to water stress simulated at Selhausen is not much larger than at Rollesbroich. One reason for
697 this is clearly the deeper root system. AnotherThe reason for this becomes apparent from a
698 comparison of the results for the two highlighted simulations in figure 8, which.Figure 8 shows
699 the simulated time-courses of the two water stress functions in the model. This comparison
700 shows that simulations with strong reductions in the dry matter allocation function have
701 correspondingly small reductions in the stress function regulating transpiration or, as in this
702 example (simulation number 6), none at all. This is because an increased rate of leaf loss and
703 a greater allocation of assimilates to the below-ground biomass during drought reduces the
704 transpiration demand as well as increasing the potential rate of water uptake by the root
705 system. These adaptation mechanisms in response to soil drying conserve soil water and
706 reduce the likelihood of stomatal closure, so that transpiration can be maintained during
707 extended dry summer periods. Shorter periods of stomatal closure induced by water stress do
708 occur every summer at Selhausen in most of the acceptable model simulations, with one more
709 extended period of drought stress (ca. 1 to 2 weeks) in 2018. However, overall, the extent and
710 severity of reductions in transpiration due to water stress simulated at Selhausen is not much
711 larger than at Rollesbroich. This comparison illustrates the fact that simulations with strong
712 reductions in the dry matter allocation function show correspondingly small reductions in the
713 stress function regulating transpiration or, as in this example (simulation number 6), none at
714 all. This is because an increased rate of leaf loss and a greater allocation of assimilates to the
715 below ground biomass during drought reduces the transpiration demand as well as increasing
716 the potential rate of water uptake by the root system. These adaptation mechanisms in
717 response to soil drying conserve soil water and reduce the likelihood of stomatal closure, so
718 that transpiration can be maintained during extended dry summer periods at Selhausen.

720 3.3 Grassland growth

721 Figures 9 and 10 show comparisons of the acceptable simulations with the measurements of
722 leaf area index and harvested biomass on the lysimeters at Selhausen and Rollesbroich. The
723 model efficiencies for these two data types are shown in table 6. Figure 11 shows box and
724 whisker plots of the simulated total harvest and overall water use efficiencies (WUE, defined
725 as total harvest divided by evapotranspiration) at the two sites. The results suggest that the
726 model performed satisfactorily for leaf area development at both sites and for harvested
727 biomass at Selhausen, but not for harvests at Rollesbroich (table 6). These poorer results can
728 largely be explained by the fact that lysimeter Ro_Y_013 was considered an outlier, so no
729 effort was made to match this data by loosening the constraints in the GLUE analysis.

730 Figure 12 shows the gain and loss terms in the dry matter balances simulated with the 30 best
731 parameterizations at each site. Simulated assimilation was ca. 10% larger at Selhausen
732 compared with Rollesbroich as a consequence of the greater radiation input and higher
733 temperatures (Figure S1) and the fact that water stress is only slightly more prevalent (Figure
734 8). Leaf loss is a relatively small term in the mass balance (10-12% of assimilation) and is similar
735 at both sites (Figure 12). Root production and decay (i.e. turnover) are more significant terms,
736 with root decay closely mirroring production, since it is modelled as a first-order function of
737 biomass. Expressed as a proportion of assimilation, simulated root production and decay is
738 somewhat larger at Selhausen compared with Rollesbroich (ca. 58 and 53% of assimilation
739 respectively, on average, for both), while root biomass is also somewhat larger at Selhausen
740 (see figure S98). This is in agreement with experimental studies that have demonstrated
741 increases in below-ground biomass production in grasslands as a consequence of drought (e.g.
742 Jones et al., 1980a; Kahmen et al., 2005; Wedderburn et al., 2010; Skinner and Comas, 2010;
743 Padilla et al., 2013; Nosalewicz et al., 2018; Meurer et al., 2019). It was not possible to make
744 measurements of root biomass and production in the lysimeters at the two sites due to the
745 constraints of the experimental set-up. However, literature data on root biomass and
746 production in similar temperate grassland environments can serve as an approximate “reality-
747 check”, suggesting that our simulations (Figure S98) are reasonable. For example, in northern
748 Germany, Chen et al. (2016) measured a root biomass of ca. 500 g m⁻² at 0-30 cm depth and a
749 growth rate of 450 g m⁻² year⁻¹, while in central Sweden, Meurer et al. (2019) found a root
750 biomass of 250-330 g m⁻² in the same depth interval. In central France, Picon-Cochard et al.
751 (2012) reported summer peak root biomasses of 13 perennial grasses grown in monoculture
752 varying between ca. 400 and 800 g m⁻², with a temporal pattern matching that simulated by
753 our model (Figure S98). Likewise, Wedderburn et al. (2010) reported peak root counts in early
754 summer and a minimum in winter for *Lolium perenne* pastures in New Zealand. The values of
755 below-ground production simulated by our model are also within the range reported by Hui
756 and Jackson (2006) for temperate grasslands in a global meta-analysis.

757 4. Conclusions

758 In this study, we made use of an eco-hydrological model to analyze the impacts on soil water
759 balance and grassland production of climate change triggered by the transfer of weighing
760 lysimeters from a wet, cool climate (Rollesbroich) to a drier, warmer climate (Selhausen). The
761 relatively simple model employed in this study gave ~~satisfactory~~excellent simulations of soil
762 water contents (Model Efficiency, ME, between 0.24 and 0.87) and evapotranspiration rates
763 (ME between 0.32 and 0.60) measured at a daily resolution at both sites during a six-year
764 period, as well as acceptable simulations of leaf area development (ME between -0.04 and
765 0.50). In this model application, we assumed identical static root distributions for the
766 grassland at the two sites and inferred different (constant) values of the maximum root depth,
767 with deeper roots in the drier climate at Selhausen. We also concluded from the modelling
768 that more frequent and intense soil drying at Selhausen led to a shift towards a greater
769 production of below-ground biomass, thus mitigating drought stress. A major challenge for
770 the future will be to further develop crop and eco-hydrological models to enable them to
771 predict these dynamic responses of plant roots to changing soil and climatic conditions as
772 emergent phenomena. In this respect, it should be worthwhile to test simple empirical

773 approaches to link root distribution with maximum root depth and biomass (e.g. Arora and
774 Boer, 2003) as well as developing improved architectural models of root growth (e.g. Postma
775 et al., 2017; Schnepf et al., 2018; Mboh et al., 2019). Regardless of modelling approach, it
776 seems clear that plastic responses of plant traits to climate change of the kind we inferred
777 from our study (e.g. in root depth or leaf conductance) introduce significant uncertainties into
778 model predictions of water balance and plant growth.

779 **Data availability**

780 The raw data can be freely obtained from the TERENO data portal ([https://teodoor.icg.kfa-
781 juelich.de/ddp/index.jsp](https://teodoor.icg.kfa-juelich.de/ddp/index.jsp)). Processed data developed during this study can be acquired upon
782 request from Jannis Groh or Katharina Meurer.

783

784 **Author contributions**

785 The study was conceived by NJ, HV, KM and EL. NJ built the model. TP, JG, WD and CB supplied
786 data and advised on its use. Initial data analyses and model applications were carried out by
787 ER as part of his thesis project, supervised by KM, NJ and EL. NJ and KM carried out the final
788 simulations. NJ prepared the manuscript with contributions from all authors.

789 **Competing interests**

790 The authors declare that they have no conflict of interest.

791 **Acknowledgments**

792 This work was partly funded by the Swedish Research Council for Sustainable Development
793 (FORMAS, grant no. 2018-02319). We also acknowledge the support of the TERENO-SoilCan
794 program funded by the Helmholtz Association (HGF) and the Federal Ministry of Education
795 and Research (BMBF). We would also like to thank Werner Küpper, Ferdinand Engels, Philipp
796 Meulendick, Rainer Harms, and Leander Fürst at the Selhausen and Rollesbroich lysimeter
797 stations for their support.

References

- Akmal, M., and Janssens, M.: Productivity and light use efficiency of perennial ryegrass with contrasting water and nitrogen supplies, *Field Crops Res.*, 88, 143-155, 2004
- Allen, R., Pereira, L., Raes, D., and Smith, M.: Crop evapotranspiration – guidelines for computing crop water requirements, FAO Irrigation and Drainage Paper 56, FAO Food and Agricultural Organization of the United Nations, Rome, 1998.
- Arora, V., and Boer, G.: A representation of variable root distribution in dynamic vegetation models, *Earth Int.*, 7, Paper no.6, 1-19, 2003.
- Ataroff, M., and Naranjo, M.: Interception of water by pastures of *Pennisetum clandestinum* Hochst. ex Chiov. and *Melinis minutiflora* Beauv. *Agric. Forest Meteor.*, 149, 1616-1620, 2009.
- ~~Bartlett, M., Zhang, Y., Kreidler, N., Sun, S., Ardy, R., Cao, K., and Sack, L.: Global analysis of plasticity in turgor loss point, a key drought tolerance trait, *Ecology Lett.*, 17, 1580-1590, 2014.~~
- Beier, C., Beierkuhnlein, C., Wohlgemuth, T., Penuelas, J., Emmett, B., Körner, C., de Boeck, H., Hesselbjerg Christensen, J., Leuzinger, S., Janssens, I., and Hansen, K.: Precipitation manipulation experiments – challenges and recommendations for the future, *Ecology Lett.*, 15, 899-911, 2012.
- Bellocchi, G., Rivington, M., Donatelli, M., and Matthews, K.: Validation of biophysical models: issues and methodologies. A review, *Agron. Sust. Dev.*, 30, 109-130, 2010.
- Benot, M-L., Morvan-Bertrand, A., Mony, C., Huet, J., Sulmon, C., Decau, M-L., Prud'homme M-P., and Bonis, A.: Grazing intensity modulates carbohydrate storage pattern in five grass species from temperate grasslands, *Acta Oecol.*, 95, 108-115, 2019.
- Beven, K., and Binley, A.: The future of distributed models: model calibration and uncertainty prediction. *Hydrol. Proc.*, 6, 279-298, 1992.
- Beven, K.: A manifesto for the equifinality thesis. *J. Hydrol.*, 320, 18-36, 2006.
- Black, A., Moot, D., and Lucas, R.: Development and growth characteristics of Caucasian and white clover seedlings, compared with perennial ryegrass, *Grass Forage Sci.*, 61, 442-453, 2006.
- Bogena, H., Montzka, C., Huisman, J., Graf, A., Schmidt, M., Stockinger, M., von Hebel, C., Hendricks-Franssen, H., van der Kruk, J., Tappe, W., Lücke, A., Baatz, R., Bol, R., Groh, J., Pütz, T., Jakobi, J., Kunkel, R., Sorg, J., and Vereecken, H.: The TERENO-Rur hydrological observatory: a multiscale multi-compartment research platform for the advancement of hydrological science, *Vadose Zone J.*, 17:180055. doi:10.2136/vzj2018.03.0055, 2018.
- Bollig, C., and Feller, U.: Impacts of drought stress on water relations and carbon assimilation in grassland species at different altitudes, *Agric., Ecosyst. Environ.*, 188, 212-220, 2014.
- Bonos, S., and Murphy, J.: Growth responses and performance of Kentucky Bluegrass under summer stress, *Crop Sci.*, 39, 770-774, 1999.
- Boote, K., Jones, J., White, J., Asseng, S., and Lizaso, J.: Putting mechanisms into crop production models, *Plant, Cell Environ.*, 36, 1658-1672, 2013.
- Bossio, D., Cook-Patton, S., Ellis, P., Fargione, J., Sanderman, J., Smith, P., Wood, S., Zomer, R., von Unger, M., Emmer, I., and Griscom, B.: The role of soil carbon in natural climate solutions, *Nature Sustainability*, doi.org/10.1038/s41893-020-0491-z, 391-398, 2020.

- Cai, G., Vanderborght, J., Couvreur, V., Mboh, C., and Vereecken, H.: Parameterization of root water uptake models considering dynamic root distributions and water uptake compensation, *Vadose Zone J.*, 17:160125. doi:10.2136/vzj2016.12.0125, 2017.
- Chen, H., and Brassard, B.: Intrinsic and extrinsic controls of fine root life span, *Crit. Rev. Plant Sci.*, 32, 151-161, 2013.
- Chen, S., Lin, S., Reinsch, T., Loges, R., Hasler, M., and Taube, F.: Comparison of ingrowth core and sequential soil core methods for estimating belowground net primary production in grass–clover swards, *Grass Forage Sci.*, 71, 515-528, 2016.
- Coleman, S., Shiel, R., and Evans, D.: The effects of weather and nutrition on the yield of hay from Palace Leas meadow hay plots, at Cockle Park experimental farm, over the period from 1897 to 1980, *Grass Forage Sci.*, 42, 353-358, 1989.
- Couvreur, V., Vanderborght, J., and Javaux, M.: A simple three-dimensional macroscopic root water uptake model based on the hydraulic architecture approach, *Hydrol. Earth Syst. Sci.*, 16, 2957-2971, 2012.
- DaCosta, M., Wang, Z., and Huang, B.: Physiological adaptation of Kentucky Bluegrass to localized soil drying, *Crop Sci.*, 44, 1307-1314, 2004.
- de Jong van Lier, Q., van Dam, J., Metselaar, K., de Jong, R., and Duijnisveld, W.: Macroscopic root water uptake distribution using a matric flux potential approach, *Vadose Zone J.*, 7, 1065-1078, 2018.
- de Jong van Lier, Q., Dourado Neto, D., and Metselaar, K.: Modeling of transpiration reduction in van Genuchten–Mualem type soils, *Water Resour. Res.*, 45, W02422, doi:10.1029/2008WR006938, 2009.
- de Jong van Lier, Q., van Dam, J., Durigon, A., dos Santos, M., and Metselaar, K.: Modeling water potentials and flows in the soil-plant system comparing hydraulic resistances and transpiration reduction functions, *Vadose Zone J.*, 12, doi: 10.2136/vzj2013.02.0039, 2013.
- de Willigen, P., van Dam, J., Javaux, M., and Heinen, M.: Root water uptake as simulated by three soil water flow models, *Vadose Zone J.*, doi:10.2136/vzj2012.0018, 2012.
- Diekkrüger, B., Söndgerath, D., Kersebaum, K., and McVoy, C.: Validity of agroecosystem models a comparison of results of different models applied to the same data set. *Ecol. Modell.*, 81, 3-29, 1995.
- Dunbabin, V., Postma, J., Schnepf, A., Pagès, L., Javaux, M., Wu, L., Leitner, D., Chen, Y., Rengel, Z., and Diggle, A.: Modelling root-soil interactions using three-dimensional models of root growth, architecture and function, *Plant Soil*, 372, 93-124, 2013.
- Eckersten, H., Herrmann, A., Kornher, A., Halling, M., Sindhøj, E., and Lewan, E.: Predicting silage maize yield and quality in Sweden as influenced by climate change and variability, *Acta Agric. Scand., Section B – Soil and Plant Sci.*, 62, 151-165, 2012.
- Fan, J., McConkey, B., Wang, H., and Janzen, H.: Root distribution by depth for temperate agricultural crops, *Field Crops Res.*, 189, 68-74, 2016.
- Faria, L., da Rocha, M., de Jong van Lier, Q., and Casaroli, D.: A split-pot experiment with sorghum to test a root water uptake partitioning model, *Plant Soil*, 331, 299-311, 2010.

- Fatichi, S., Pappas, C., and Ivanov, V.: Modeling plant-water interactions: an ecohydrological overview from the cell to the global scale, *WIREs Water* 3, 327-368. doi: 10.1002/wat2.1125, 2016.
- Foley, J., Ramankutty, N., Brauman, K., Cassidy, E., Gerber, J., Johnston, M., Mueller, N., O'Connell, C., Ray, D., West, P., Balzer, C., Bennett, E., Carpenter, S., Hill, J., Monfreda, C., Polasky, S., Rockström, J., Sheehan, J., Siebert, S., Tilman, D., and Zaks, D.: Solutions for a cultivated planet, *Nature* 7369, 337-342, 2011.
- Forstner, V., Groh, J., Vremec, M., Herndl, M., Vereecken, H., Gerke, H. H., Birk, S., and Pütz, T.: Response of water fluxes and biomass production to climate change in permanent grassland soil ecosystems, *Hydrol. Earth Syst. Sci.*, 25, 6087–6106
- Friedlingstein, P., Joel, G., Field, C., and Fung, I.: Toward an allocation scheme for global terrestrial carbon models, *Global Change Biology*, 5, 755-770, 1999.
- Gebler, S., Hendricks Franssen, H-J., Pütz, T., Post, H., Schmidt, M., and Vereecken, H.: Actual evapotranspiration and precipitation measured by lysimeters: a comparison with eddy covariance and tipping bucket. *Hydrol. Earth Syst. Sci.*, 19, 2145-2161, 2015.
- Gifford, R.: Plant respiration in productivity models: conceptualisation, representation and issues for global terrestrial carbon-cycle research, *Funct. Plant Biol.*, 30, 171-186, 2003.
- Giraud, M., Groh, J., Gerke, H. H., Brüggemann, N., Vereecken, H., and Pütz, T.: Soil nitrogen dynamics in a managed temperate grassland under changed climatic conditions, *Water*, 13, 931, doi.org/10.3390/w13070931, 2021.
- Groh, J., Pütz, T., Gerke, H., Vanderborght, J., and Vereecken, H.: Quantification and prediction of nighttime evapotranspiration for two distinct grassland ecosystems. *Water Resour. Res.*, 55, 2961-2975, 2019.
- Groh, J., Diamantopoulos, E., Duan, X., Ewert, F., Herbst, M., Holbak, M., Kamali, B., Kersebaum, K.-C., Kuhnert, M., Lischeid, G., Nendel, C., Priesack, E., Steidl, J., Sommer, M., Pütz, T., Vereecken, H., Wallor, E., Weber, T., Wegehenkel, M., Weihermüller, L., and Gerke, H.: Crop growth and soil water fluxes at erosion-affected arable sites: using weighing lysimeter data for model intercomparison, *Vadose Zone J.*, 19: e20058. doi:10.1002/vzj2.20058, 2020a.
- Groh, J., Vanderborght, J., Pütz, T., Vogel, H-J., Gründling, R., Rupp, H., Rahmati, M., Sommer, M., Vereecken, H., and Gerke, H.: Responses of soil water storage and crop water use efficiency to changing climatic conditions: a lysimeter-based space-for-time approach. *Hydrol. Earth Syst. Sci.*, 24, 1211-1225, 2020b.
- Guest, G., Kröbel, R., Grant, B., Smith, W., Sansoulet, J., Pattey, E., Desjardins, R., Jégo, G., Tremblay, N., and Tremblay, G.: Model comparison of soil processes in eastern Canada using DayCent, DNDC and STICS, *Nutr. Cycl. Agroecosyst.*, 109, 211-232, 2017.
- Gupta, A., Rico Medina, A., and Caño Delgado, A.: The physiology of plant responses to drought. *Science*, 266-269, 2020.
- He, D, Wang, E., Wang, J., and Robertson, M.: Data requirement for effective calibration of process-based crop models. *Agric. Forest Meteorol.*, 234-235, 136-148, 2017.
- Heinlein, F., Biernath, C., Klein, C., Thieme, C., and Priesack, E.: Evaluation of simulated transpiration from maize plants on lysimeters, *Vadose Zone J.*, doi:10.2136/vzj2016.05.0042, 2017.

- Hennessy, D., O'Donovan, M., French, P., and Laidlaw, A.: Factors influencing tissue turnover during winter in perennial ryegrass-dominated swards, *Grass Forage Sci.*, 63, 202–211, 2008.
- Hofer, D., Suter, M., Buchmann, N., and Lüscher, A.: Severe water deficit restricts biomass production of *Lolium perenne* L. and *Trifolium repens* L. and causes foliar nitrogen but not carbohydrate limitation. *Plant Soil*, 421, 367-380, 2017.
- Hoover, D., Wilcox, K., and Young, K.: Experimental droughts with rainout shelters: a methodological review, *Ecosphere* 9(1):e02088. 10.1002/ecs2.2088, 2018.
- Howard, H., and Watschke, T.: Variable high-temperature tolerance among Kentucky Bluegrass cultivars. *Agron. J.*, 83, 689-693, 1991.
- Hu, Z., Yu, G., Zhou, Y., Sun, X., Li, Y., Shi, P., Wang, Y., Song, X., Zheng, Z., Zhang, L., and Li, S.: Partitioning of evapotranspiration and its controls in four grassland ecosystems: application of a two-source model. *Agric. Forest Meteor.*, 149, 1410-1420, 2009.
- Hui, D., and Jackson, R.: Geographical and interannual variability in biomass partitioning in grassland ecosystems: a synthesis of field data, *New Phytol.*, 169, 85–93, 2006.
- Ineson, P., Taylor, K., Harrison, A., Poskitt, J., Benham D., Tipping, E., and Woof C.: Effects of climate change on nitrogen dynamics in upland soils. 1. A transplant approach, *Global Change Biol.*, 4, 143-152, 1998.
- Istanbulluoglu, E., Wang, T., and Wedin, D.: Evaluation of ecohydrologic model parsimony at local and regional scales in a semiarid grassland ecosystem, *Ecohydrol.*, 5, 121-142, 2012.
- Jackson, R., Canadell, J., Ehleringer, J., Mooney, H., Sala, O., and Schulze, E.: A global analysis of root distributions for terrestrial biomes, *Oecologia*, 108, 389–411, 1996.
- Javaux, M., Couvreur, V., Vanderborght, J., and Vereecken, H.: Root water uptake: from three-dimensional biophysical processes to macroscopic modeling approaches, *Vadose Zone J.*, doi:10.2136/vzj2013.02.0042, 2013.
- Jarvis, N.: Simple physics-based models of compensatory plant water uptake: concepts and ecohydrological consequences. *Hydrol. Earth Syst. Sci.*, 15, 3431-3446, 2011.
- Jarvis, N., Koestel, J., Messing, I., Moeys, J., and Lindahl, A.: Influence of soil, land use and climatic factors on the hydraulic conductivity of soil. *Hydrol. Earth Syst. Sci.*, 17, 5185-5195, 2013.
- Jenkinson, D., Potts, J., Perry, J., Barnett, V., Coleman, K., and Johnston, A.: Trends in herbage yields over the last century on the Rothamsted long-term continuous hay experiment, *J. Agric. Sci.*, 122, 365-374, 1994.
- Jing, Q., Bélanger, G., Baron, V., Bonesmo, H., Virkajärvi, P., and Young, D.: Regrowth simulation of the perennial grass timothy, *Ecol. Modell.*, 232, 64-77, 2012.
- Johansson, G.: Carbon distribution in grass (*Festuca pratensis* L.) during regrowth after cutting-utilization of stored and newly assimilated carbon, *Plant Soil*, 151, 11-20, 1993.
- [Johnson, I., Chapman, D., Snow, V., Eckard, R., Parsons, A., Lambert, M., and Cullen, B.: DairyMod and EcoMod: biophysical pasture-simulation models for Australia and New Zealand. *Aust. J. Exp. Agric.*, 48, 621-631, 2008.](#)

- Jones, M., Leafe, E., and Stiles, W.: Water stress in field-grown perennial ryegrass I. Its effect on growth, canopy photosynthesis, and transpiration, *Ann. Appl. Biol.*, 96, 87-101, 1980a.
- Jones, M., Leafe, E., and Stiles, W.: Water stress in field-grown perennial ryegrass I. Its effect on leaf water status, stomatal-resistance, and leaf morphology, *Ann. Appl. Biol.*, 96, 103-110, 1980b.
- Jouven, M., Carrère, P., and Baumont, R.: Model predicting dynamics of biomass, structure and digestibility of herbage in managed permanent pastures. 1. Model description, *Grass Forage Sci.*, 61, 112–124, 2006a.
- Jouven, M., Carrère, P., and Baumont, R.: Model predicting dynamics of biomass, structure and digestibility of herbage in managed permanent pastures. 1. Model evaluation, *Grass Forage Sci.*, 61, 125–133, 2006b.
- Jupp, A., and Newman, E.: Morphological and anatomical effects of severe drought on the roots of *Lolium perenne* L., *New Phytol.*, 105, 393-402, 1987.
- Kahmen, A., Perner, J., and Buchmann, N.: Diversity-dependent productivity in semi-natural grasslands following climate perturbations, *Func. Ecol.*, 19, 594-601, 2005.
- Katata, G., Grote, R., Mauder, M., Zeeman, M., and Ota, M.: Wintertime grassland dynamics may influence belowground biomass under climate change: a model analysis, *Biogeosci.*, 17, 1071-1085, 2020.
- Kellner, J., Multsch, S., Houska, T., Kraft, P., Müller, C., and Breuer, L.: A coupled hydrological-plant growth model for simulating the effect of elevated CO₂ on a temperate grassland, *Agric. Forest Meteorol.*, 246, 42-50, 2017.
- Kemp, D., and Culvenor, R.: Improving the grazing and drought tolerance of temperate perennial grasses, *New Zealand J. Agric. Res.*, 37, 365-378, 1994.
- Kersebaum K., Hecker, J., Mirschel W., Wegehenkel M. 2007. Modelling water and nutrient dynamics in soil–crop systems: a comparison of simulation models applied on common data sets. In: Kersebaum, K., Hecker, J., Mirschel, W., Wegehenkel, M. (eds.) Modelling water and nutrient dynamics in soil–crop systems. Springer, Dordrecht.
- Kersebaum, K., Boote, K., Jorgenson, J., Nendel, C., Bindi, M., Frühauf, C., Gaiser, T., Hoogenboom, G., Kollas, C., Olesen, J., Rötter, R., Ruget, F., Thorburn, P., Trnka, M., and Wegehenkel, M.: Analysis and classification of data sets for calibration and validation of agro-ecosystem models, *Environ. Modell. & Softw.*, 72, 402-417, 2015.
- Kipling, R., Virkajärvi, P., Breitsameter, L., Curnel, Y., De Swaef, T., Gustavsson, A-M., Hennart, S., Höglind, M., Järvenranta, K., Minet, J., Nendel, C., Persson, T., Picon-Cochard, C., Rolinski, S., Sandars, D., Scollan N., Sebek, L., Seddaiu, G., Topp, C., Twardy, S., Van Middelkoop, J., Wu, L., and Bellocchi, G.: Key challenges and priorities for modelling European grasslands under climate change, *Sci. Tot. Environ.*, 566–567, 851–864, 2016.
- Kirchner, J.: Getting the right answers for the right reasons: linking measurements, analyses, and models to advance the science of hydrology, *Water Resour. Res.*, 42, W03S04, doi: <https://doi.org/10.1029/2005WR004362>, 2006.
- Klein, C., Biernath, C., Heinlein, F., Thieme, C., Gilgen, A., Zeeman, M., and Priesack, E.: Vegetation growth models improve surface layer flux simulations of a temperate grassland, *Vadose Zone J.*, 16, doi:10.2136/vzj2017.03.0052, 2017.

- Körner, C.: Winter crop growth at low temperature may hold the answer for alpine treeline formation. *Plant Ecol. & Divers.*, 1, 3-11, 2008.
- Körner, C.: Paradigm shift in plant growth control. *Current Opinion Plant Biol.*, 25, 107–114, 2015.
- Kröbel, R., Sun, Q., Ingwersen, J., Chen, X., Zhang, F., Müller, T., and Römheld, V.: Modelling water dynamics with DNDC and DAISY in a soil of the North China Plain: a comparative study, *Environ. Modell. & Softw.*, 25, 583-601, 2010.
- Li, W., Ciais, P., Guenet, B., Peng, S., Chang, J., Chaplot, V., Khudyaev, S., Peregon, A., Piao, S., Wang, Y., and Yue, C.: Temporal response of soil organic carbon after grassland-related land-use change, *Global Change Biol.*, 24, 4731-4746, 2018.
- Loka, D., Harper, J., Humphreys, M., Gasior, D., Wootton-Beard, P., Gwynn-Jones, D., Scullion, J., John Doonan, J., Kingston-Smith, A., Dodd, R., Wang, J., Chadwick, D., Hill, P., Jones, D., Mills, G., Hayes, F., and Robinson, D.: Impacts of abiotic stresses on the physiology and metabolism of cool-season grasses: a review, *Food & Energy Security*, 8:e00152, 2019.
- Luckner, L., van Genuchten, M., and Nielsen, D.: A consistent set of parametric models for the two-phase flow of immiscible fluids in the subsurface, *Water Resour. Res.*, 25, 2187– 2193, 1989.
- Ma, S., Lardy, R., Graux, A-I., Ben Touhami, H., Klumpp, K., Martin, R., and Bellocchi, G.: Regional-scale analysis of carbon and water cycles on managed grassland systems, *Environ. Modell. & Softw.*, 72, 356-371, 2015.
- ~~Manzoni, S., Vico, G., Porporato, A., and Katul, G.: Biological constraints on water transport in the soil-plant-atmosphere system, *Adv. Water Resour.*, 51, 292-304, 2013.~~
- Martínez-Vilalta, J., Sala, A., Asensio, D., Galiano, L., Hoch, G., Palacio, S., Piper F., and Lloret, F.: Dynamics of non-structural carbohydrates in terrestrial plants: a global synthesis, *Ecol. Monogr.*, 86, 495-516, 2016.
- ~~Maseda, P., and Fernández, R.: Stay wet or else: three ways in which plants can adjust hydraulically to their environment, *J. Exp. Bot.*, 57, 3963-3977, 2006.~~
- Mboh, C., Srivastava, A., Gaiser, T., and Ewert, F.: Including root architecture in a crop model improves predictions of spring wheat grain yield and above-ground biomass under water limitations. *J. Agron. Crop Sci.*, 205, 109-128, 2019.
- Metselaar, K., Pinheiro, E., and de Jong van Lier, Q.: Mathematical description of rooting profiles of agricultural crops and its effect on transpiration prediction by a hydrological model, *Soil Syst.*, 3, 44, doi:10.3390/soilsystems3030044, 2019.
- Meurer, K., Bolinder, M., Andren, O., Hansson, A-C., Pettersson, R., and Kätterer, T.: Shoot and root production in mixed grass ley under daily fertilization and irrigation: validating the N productivity concept under field conditions, *Nutr. Cycl. Agroecosyst.*, 115, 85-99, 2019.
- Meurer, K., Chenu, C., Coucheney, E., Herrmann, A., Keller, T., Kätterer, T., Nimblad Svensson, D., and Jarvis, N.: Modelling dynamic interactions between soil structure and the storage and turnover of soil organic matter. *Biogeosci.*, 17, 5025-5042, 2020.
- Montaldo, N., Rondena, R., Albertson, J., and Mancini, M.: Parsimonious modeling of vegetation dynamics for ecohydrologic studies of water-limited ecosystems. *Water Resour. Res.*, 41, W10416, doi:10.1029/2005WR004094, 2005.

- Monteith, J.: How do crops manipulate water supply and demand? *Phil. Trans. Royal Soc. London A*, 316, 245-259, 1986.
- Monteith, J.: Does transpiration limit the growth of vegetation or vice versa? *J. Hydrol.*, 100, 57-68, 1988.
- Morvan-Bertrand, A., Pavis, N., Boucaud, J., and Prud'homme M-P.: Partitioning of reserve and newly assimilated carbon in roots and leaf tissues of *Lolium perenne* during regrowth after defoliation: assessment by ¹³C steady-state labelling and carbohydrate analysis, *Plant Cell Environ.*, 22, 1097–1108, 1999.
- Mualem, Y.: New model for predicting hydraulic conductivity of unsaturated porous-media, *Water Resour. Res.*, 12, 513-522, 1976.
- ~~Nicotra, A., and Davidson, A.: Adaptive phenotypic plasticity and plant water use, *Funct. Plant Biol.*, 37, 117-127, 2010.~~
- Nicotra, A., Atkin, O., Bonser, S., Davidson, A., Finnegan, E., Mathesius, U., Poot, P., Purugganan, M., Richards, C., Valladares, F., and van Kleunen, M.: Plant phenotypic plasticity in a changing climate, *Trends Plant Sci.*, 15, 684-692, 2010.
- Norris, I.: Soil moisture and growth of contrasting varieties of *Lolium*, *Dactylis* and *Festuca* species, *Grass Forage Sci.*, 37, 273-283, 1982.
- Nosalewicz, A., Siecińska, J., Kondracka, K., and Nosalewicz, M.: The functioning of *Festuca arundinacea* and *Lolium perenne* under drought is improved to a different extend by the previous exposure to water deficit, *Environ. Exp. Bot.*, 156, 271-278, 2018.
- Østrem, L., Rapacz, M., Jørgensen, M., and Höglind, M.: Effect of developmental stage on carbohydrate accumulation patterns during winter of timothy and perennial ryegrass, *Acta Agric. Scand. Section B – Soil Plant Sci.*, 61, 153-163, 2011.
- Padilla, F., Aarts, B., Roijendijk, Y., de Caluwe, H., Mommer, L., Visser, E., and de Kroon, H.: Root plasticity maintains growth of temperate grassland species under pulsed water supply, *Plant Soil*, 369, 377-386, 2013.
- Persson, T., Höglind, M., Gustavsson, A-M., Halling, M., Jauhiainen, L., Niemeläinen, O., Thorvaldsson, G., and Virkajärvi, P.: Evaluation of the LINGRA timothy model under Nordic conditions, *Field Crops Res.*, 161, 87-97, 2014.
- Peters, A., Groh, J., Schrader, F., Durner, W., Vereecken, H., and Pütz, T.: Towards an unbiased filter routine to determine precipitation and evapotranspiration from high precision lysimeter measurements, *J. Hydrol.*, 549, 731-740, 2017.
- Picon-Cochard, C., Pilon, R., Tarroux, E., Pagès, L., Robertson, J., and Dawson, L.: Effect of species, root branching order and season on the root traits of 13 perennial grass species, *Plant Soil*, 353, 47-57, 2012.
- Postma, J., Kuppe, C., Owen, M., Mellor, N., Griffiths, M., Bennett, M., Lynch, J., and Watt, M.: OPENSIMROOT: widening the scope and application of root architectural models, *New Phytol.*, 215, 1274-1286, 2017.

- Pütz, T., Kiese, R., Wollschläger, U., Groh, J., Rupp, H., Zacharias, S., Priesack, E., Gerke, H., Gasche, R., Bens, O., Borg, E., Baessler, C., Kaiser, K., Herbrich, M., Munch, J.-C., Sommer, M., Vogel, H.-J., Vanderborght, J., and Vereecken, H.: TERENO-SOILCan: a lysimeter-network in Germany observing soil processes and plant diversity influenced by climate change. *Environ. Earth Sci.*, 75, 1242, 2016.
- Raats, P.: Uptake of water from soils by plant roots. *Transport Porous Med.*, 68, 5-28, 2007.
- Rahmati, M., Groh, J., Graf, A., Pütz, T., Vanderborght, J., and Vereecken, H.: On the impact of increasing drought on the relationship between soil water content and evapotranspiration of a grassland, *Vadose Zone J.*, doi: 10.1002/vzj2.20029, 2020.
- Robertson, M., Rebetzke, G., and Norton, R.: Assessing the place and role of crop simulation modelling in Australia, *Crop Pasture Sci.*, 66, 877-893, 2015.
- [Robinson, D., Hopmans, J., Filipovic, V., van der Ploeg, M., Lebron, I., Jones, S., Reinsch, S., Jarvis, N., and Tuller, M.: Gobar environmental changes impact soil hydraulic functions through biophysical feedbacks. *Global Change Biol.*, 25, 1895-1904, 2019.](#)
- Ruane, A., Phillips, M., and Rosenzweig, C.: Climate shifts within major agricultural seasons for +1.5 and +2.0°C worlds: HAPPI projections and AgMIP modeling scenarios, *Agric. Forest Meteorol.*, 259, 329-344, 2018.
- [Sadok, W., Lopez, J., and Smith, K.: Transpiration increases under high-temperature stress: potential mechanisms, trade-offs and prospects for crop resilience in a warming world. *Plant Cell Environ.*, 44, 2102-2116, 2021.](#)
- Sándor, R., Barcza, Z., Acutis, M., Doro, L., Hidy, D., Köchy, M., Minet, J., Lellei-Kovács, E., Ma, S., Perego, A., Rolinski, S., Ruget, F., Sanna, M., Seddaiu, G., Wu, L., and Bellocchi, G.: Multi-model simulation of soil temperature, soil water content and biomass in Euro-Mediterranean grasslands: uncertainties and ensemble performance, *Eur. J. Agron.*, 88, 22-40, 2017.
- Schapendonk, A., Stol, W., van Kraalingen, D., and Bouman, B.: LINGRA, a sink/source model to simulate grassland productivity in Europe, *Eur. J. Agron.*, 9, 87-100, 1998.
- Schenk, H., and Jackson, R.: The global biogeography of roots, *Ecol. Monogr.*, 73, 311-328, 2002.
- Schmitt, A., Pausch, J., and Kuzyakov, Y.: Effect of clipping and shading on C allocation and fluxes in soil under ryegrass and alfalfa estimated by ¹⁴C labelling, *Appl. Soil Ecol.*, 64, 228-236, 2013.
- Schnepf, A., Leitner, D., Landl, M., Lobet, G., Mai, T-H., Morandage, S., Sheng, C., Zorner, M., Vanderborght, J., and Vereecken, H.: CRootBox: a structural-functional modelling framework for root systems, *Ann. Bot.*, 121, 1033-1053, 2018.
- Seidel, S., Palosuo, T., Thorburn, P., and Wallach, D.: Towards improved calibration of crop models – where are we now and where should we go? *Eur. J. Agron.*, 94, 25-35, 2018.
- Shuttleworth, W., and Wallace, J.: Evaporation from sparse crops – an energy combination approach. *Quart. J. Royal Meteor. Soc.*, 111, 839-855, 1985.
- Shuttleworth, W., and Gurney, R.: The theoretical relationship between foliage temperature and canopy resistance in sparse crops. *Quart. J. Royal Meteor. Soc.*, 116, 497–519, 1990.
- Silvertown, J., Dodd, M., McConway, K., Potts, J., and Crawley, M.: Rainfall, biomass variation, and community composition in the Park Grass experiment, *Ecology*, 75, 2430-2437, 1994.
- Sinclair, T., and Muchow, R.: Radiation use efficiency, *Adv. Agron.*, 65, 215-265, 1999.

- Skinner, R., and Comas, L.: Root distribution of temperate forage species subjected to water and nitrogen stress, *Crop Sci.*, 50, 2178-2185, 2010.
- Smithwick, E., Lucash, M., McCormack, M., and Sivandran, G.: Improving the representation of roots in terrestrial models, *Ecol. Modell.*, 291, 193-204, 2014.
- Staniak, M., and Kocoń, A.: Forage grasses under drought stress in conditions of Poland, *Acta Physiol. Plant.*, 37:116 DOI 10.1007/s11738-015-1864-1, 2015
- Stanimirova, R., Arévalo, P., Kaufmann, R., Maus, V., Lesiv, M., Havlík, P., and Friedl, M.: Sensitivity of global pasturelands to climate variation, *Earth's Future*, 7, 1353-1366, 2019.
- Stöckle, C., and Kemanian, A.: Can crop models identify critical gaps in genetics, environment, and management interactions? *Front. Plant Sci.*, 11, 737. doi: 10.3389/fpls.2020.00737, 2020
- Sulis, M., Couvreur, V., Keune, J., Cai, G., Trebs, I., Junk, J., Shrestha, P., Simmer, C., Kollet, S., Vereecken, H., and Vanderborght, J.: Incorporating a root water uptake model based on the hydraulic architecture approach in terrestrial systems simulations, *Agric. Forest Meteorol.*, 269-270, 28-45, 2019.
- Tardieu, F., and Parent, B.: Predictable 'meta-mechanisms' emerge from feedbacks between transpiration and plant growth and cannot be simply deduced from short-term mechanisms, *Plant Cell Environ.*, 40, 846-857, 2017.
- Tardieu, F., Draye, X., and Javaux, M.: Root water uptake and ideotypes of the root system: whole-plant controls matter, *Vadose Zone J.*, 16, doi:10.2136/vzj2017.05.0107, 2017.
- Tardieu, F., Simonneau, T., and Muller, B.: The physiological basis of drought tolerance in crop plants: a scenario-dependent probabilistic approach, *Ann. Rev. Plant Biol.*, 69, 733–759, 2018.
- Thomas, H.: Accumulation and consumption of solutes in swards of *Lolium perenne* during drought and after rewatering, *New Phytol.*, 118, 35-48, 1991.
- Thomas, H., and James, A.: Partitioning of sugars in *Lolium perenne* (perennial ryegrass) during drought and on rewatering, *New Phytol.*, 142, 295-305, 1999.
- Tubiello, F., Soussana, J., and Howden, S.: Crop and pasture response to climate change, *Proc. Natl. Acad. Sci. USA*, 104, 19686–19690, 2007.
- van der Krift, T., and Berendse, F.: Root life spans of four grass species from habitats differing in nutrient availability, *Funct. Ecol.*, 16, 198-203, 2002.
- van Genuchten, M.: A closed-form equation for predicting the hydraulic conductivity of unsaturated soils, *Soil Sci. Soc. Am. J.*, 44, 892–898, 1980.
- Vincent, C., Rowland, D., Schaffer, B., Bassil, E., Racette, K., and Zurweller, B.: Primed acclimation: a physiological process offers a strategy for more resilient and irrigation-efficient crop production, *Plant Sci.*, 295, 110240, 2020.
- Volaire, F., Thomas, H., and Lelievre F.: Survival and recovery of perennial forage grasses under prolonged Mediterranean drought I. Growth, death, water relations and solute content in herbage and stubble, *New Phytol.*, 140, 439-449, 1998.
- Wang, E., and Smith, C.: Modelling the growth and water uptake function of plant root systems: a review, *Aust. J. Agric. Res.*, 55, 501-523, 2004.

- Wedderburn, M., Crush, J., Pengelly, W., and Walcroft, J.: Root growth patterns of perennial ryegrasses under well-watered and drought conditions, *New Zealand J. Agric. Res.*, 53, 377-388, 2010.
- Wegehenkel, M., Zhang, Y., Zenker, T., and Diestel, H. The use of lysimeter data for the test of two soil–water balance models: a case study, *J. Plant Nutr. Soil Sci.*, 171, 762-776, 2008.
- White, A., Rogers, A., Rees, M., and Osborne, C.: How can we make plants grow faster? A source-sink perspective on growth rate, *J. Exp. Bot.*, 67, 31-45, 2016.
- Wingler, A.: Comparison of signaling interactions determining annual and perennial plant growth in response to low temperature, *Front. Plant Sci.*, 5, 794, doi: 10.3389/fpls.2014.00794, 2015.
- Wösten J., Lilly, A., Nemes, A., and Le Bas, C.: Development and use of a database of hydraulic properties of European soils. *Geoderma*, 90, 169-185, 1999.
- Wu, A., Song, Y., van Oosterom, E., and Hammer, G.: Connecting biochemical photosynthesis models with crop models to support crop improvement, *Front. Plant Sci.* 7:1518. doi: 10.3389/fpls.2016.01518, 2016.
- Zacharias, S., Bogen, H., Samaniego, L., Mauder, M., Fuß, R., Pütz, T., Frenzel, M., Schwank, M., Baessler, C., Butterbach-Bahl, K., Bens, O., Borg, E., Brauer, A., Dietrich, P., Hajnsek, I., Helle, G., Kiese, R., Kunstmann, H., Klotz, S., Munch, J-C., Papen H., Priesack, E., Schmid, H-P., Steinbrecher, R., Rosenbaum, U., Teutsch, G., and Vereecken, H.: A network of terrestrial environmental observatories in Germany, *Vadose Zone J.*, 10, 955-973, 2011.
- Zhang, L., Hu, Z., Fan, J., Zhou, D., and Tang, F.: A meta-analysis of the canopy light extinction coefficient in terrestrial ecosystems, *Front. Earth Sci.*, 8, 599-609, 2014.
- Zhou, M., Ishidaira, H., Hapuarachchi, H., Magome, J., Kiem, A., and Takeuchi, K.: Estimating potential evapotranspiration using Shuttleworth–Wallace model and NOAA-AVHRR NDVI data to feed a distributed hydrological model over the Mekong River basin. *J. Hydrol.*, 327, 151-173, 2006.
- Zwicke, M., Picon-Cochard, C., Morvan-Bertrand, A., Prud'homme, M-P., and Volaire, F.: What functional strategies drive drought survival and recovery of perennial species from upland grassland? *Ann. Bot.*, 116, 1001-1015, 2015.

Table 1. Soil properties at Rollesbroich

Depth (cm)	Particle size distribution (%), fine earth fraction			Texture class (U.S.D.A.)	Organic carbon (%)	pH (CaCl ₂)
	Clay (<2 μm)	Silt (2-50 μm)	Sand (50-2000μm)			
0-7	19	14	67	Sandy loam	5.3	5.2
7-24	9	33	58	Sandy loam	2.5	5.3
24-42	37	23	40	Clay loam	1.2	5.4
42-50	35	33	32	Clay loam	0.8	5.4
50-71	32	32	36	Clay loam	0.3	5.4
71-93	32	32	36	Clay loam	0.3	5.2
93-127	17	24	59	Sandy loam	0.1	4.6
127+	22	30	48	Loam	0.2	4.9

Table 2. Measured water balance, harvested biomass and water use efficiency for the lysimeters (annual averages for the period 2013-2018; P = precipitation, PET = potential evapotranspiration calculated with the FAO Penman-Monteith method, AET = actual evapotranspiration, ΔS is the change of water storage calculated as P-AET-Percolation and WUE is water use efficiency defined as harvested biomass (Harvest) divided by AET).

Site	Lysimeter	P	PET	AET	Percolation	ΔS	Harvest	WUE
		[mm/year]					[g DM m ⁻² year ⁻¹]	[kg DM m ⁻³ water]
Rollesbroich	Ro1	1055		649	438	-31	732	1.13
	Ro3	1079	710	651	466	-38	907	1.39
	Ro5	1050		623	422	5	678	1.09
	Average	1062		641	442	-21	772	1.20
Selhausen	Se21	696		716	-42	22	691	0.97
	Se25	690	827	709	-58	38	665	0.94
	Se26	699		714	-14	-1	661	0.93
	Average	695		713	-38	20	672	0.94

Table 3. Soil hydraulic parameters used in the modelling

Depths (cm)	Parameter					
	θ_s (m ³ m ⁻³)		α (cm ⁻¹)	n (-)	K_{10} (cm h ⁻¹)	τ (-)
	Selhausen	Rollesbroich				
0-24	0.45	0.55	0.025	1.34	1.89	0.5
24-48	0.39	0.39	0.025	1.09	0.73	0.5
48-90	0.38	0.38	0.025	1.08	0.83	0.5
90-140	0.38	0.38	0.025	1.17	1.46	0.5

Table 4. Fixed values for plant parameters at both sites

Parameter	Value	Sources/comments
<i>Above-ground parameters</i>		
Maximum radiation use efficiency, RUE_{max} ($MJ\ m^{-2}\ d^{-1}$)	1.6	¹ Akmal and Janssens (2004)
Leaf loss coefficient, k_{ag} (d^{-1})	0.02	Istanbulluoglu et al. (2012)
Specific leaf area, S_{leaf} ($cm^2\ g^{-1}$)	142	Site data
Base temperature, T_b ($^{\circ}C$) for stomatal conductance and assimilation	0	² Wingler (2015), Körner (2008, 2015)
Base temperature, T_b ($^{\circ}C$) for DM allocation and leaf loss	5	² Schapendonk et al. (1998), Black et al. (2006), Hennessy et al. (2008)
Optimum temperatures, $T_{o(low)}$, $T_{o(high)}$ ($^{\circ}C$) Ceiling temperature T_c ($^{\circ}C$)	12, 25 35	Howard and Watschke (1991), Wu et al. (2016), Loka et al. (2019)
Limiting soil water pressure head for cessation of transpiration, ψ_w (m)	-150	Standard assumption
Fraction of assimilates allocated to roots under optimal conditions, $f_{bg(opt)}$ (-)	0.5	Hui and Jackson (2006)
<i>Below-ground parameters</i>		
Root decay constant, k_{bg} (d^{-1})	0.007	Van der Krift and Berendse (2002), Chen and Brassard (2013)
Root radius, r_o (cm)	0.02	Van der Krift and Berendse (2002), Picon-Cochard et al. (2012)
Effective root fraction, ε (-)	0.05	Faria et al. (2010)
Specific root length, S_{root} ($m\ g^{-1}$)	118	Picon-Cochard et al. (2012)
Shape factor for root distribution, c (-)	-1.2	Schenk and Jackson (2002), Fan et al. (2016)

¹ assuming PAR = 50% of incoming solar radiation

² transpiration/assimilation is less sensitive to low temperatures than growth

Table 5. Uncertain parameters: initial ranges, data sources and ~~posterior-priori~~ parameter ranges

Parameter	Ranges sampled	Posterior-priori parameter values (n=30)					
		Selhausen			Rollesbroich		
		Median	Inter-quartile range	10 th , 90 th percentiles	Median	Inter-quartile range	10 th , 90 th percentiles
Radiation extinction coefficient, β	¹ 0.4-0.8	0.57	0.51-0.65	0.48, 0.71	0.58	0.51-0.65	0.48, 0.71
Maximum stomatal conductance, $k_{sto(max)}$ (cm s ⁻¹)	² 0.4-1.6	1.28	1.13-1.47	0.97, 1.56	0.60	0.48-0.83	0.46, 0.96
Maximum root depth, D_r (cm)	³ 40-100	79	75-83	70, 86	56	48-67	42, 73
Limiting pressure head at the root surface, $\psi_{o(crit)}$ (-cm)	⁴ 100-2000	271	233-347	195, 533	271	224-347	157, 419

¹ Schapendonk et al. (1998), Akmal and Janssens (2004), White and Snow (2012), Zhang et al. (2014)

² Nijs et al. (1997), Allen et al. (1998), Wang and Huang, (2003), DaCosta et al. (2004), Dong et al. (2011), Holloway-Phillips and Brodrigg (2011), Hu et al., 2013

³ Site observations; Jackson et al. (1996), Schenk and Jackson (2002), Fan et al. (2016)

⁴ No information is available, hence a wide 'a priori' uncertainty range was selected

Table 6. Model efficiencies for the different data types (median values of the 30 acceptable parameter sets, with minimum and maximum values in parentheses).

Site	Model efficiency					
	Water content at 10cm depth	Water content at 30 cm depth	Water content at 50 cm depth	Evapo-transpiration	Harvest	Leaf area index
Ro	0.84 (0.78, 0.87)	0.77 (0.58, 0.83)	0.73 (0.64, 0.86)	0.58 (0.54, 0.60)	-0.70 (-0.54, -0.81)	0.19 (0.09, 0.50)
Se	0.81 (0.75, 0.84)	0.68 (0.58, 0.73)	0.28 (0.24, 0.31)	0.38 (0.32, 0.45)	0.35 (0.15, 0.46)	0.15 (-0.04, 0.32)

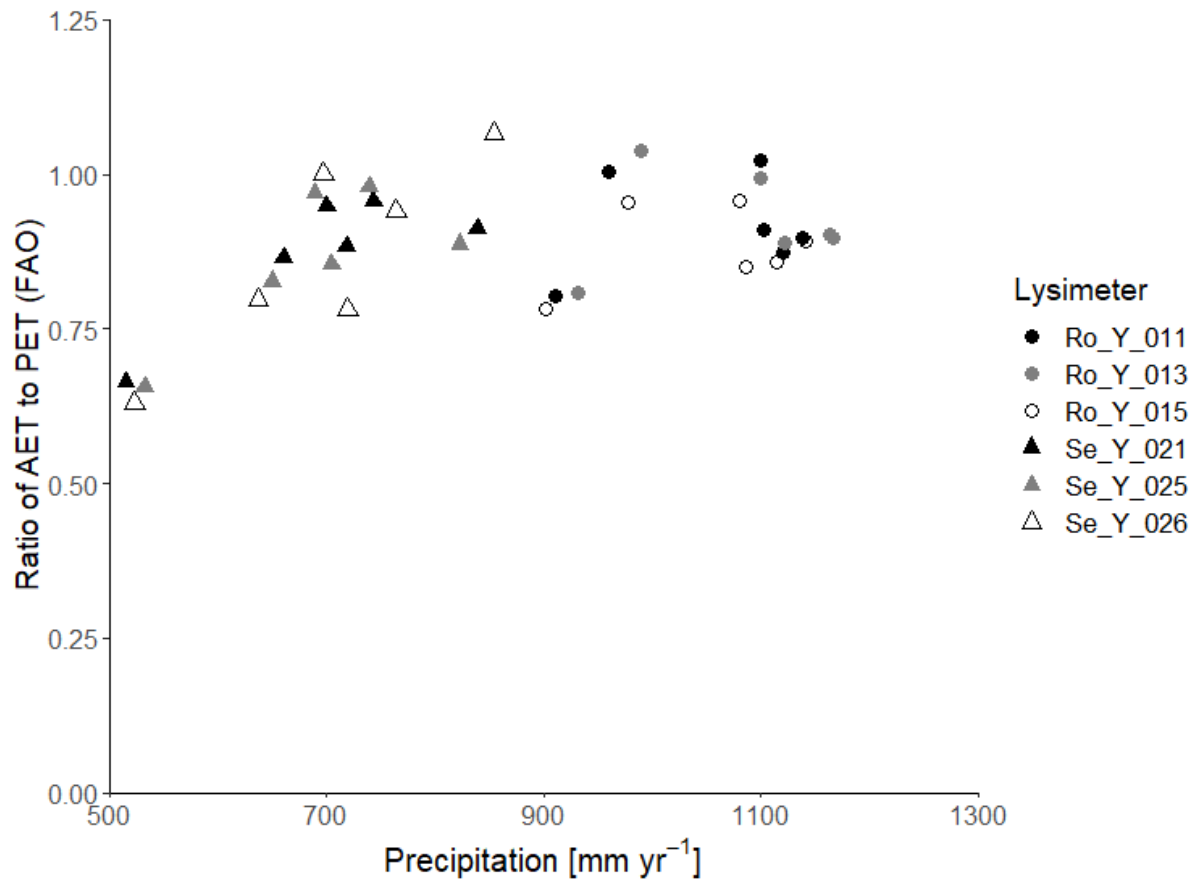


Figure 1. Ratio of actual evapotranspiration (AET) to potential evapotranspiration (PET-FAO) calculated with the FAO Penman-Monteith method (Allen et al., 1998) as a function of precipitation at Selhausen and Rollesbroich on an annual basis for the period 2013-2018.

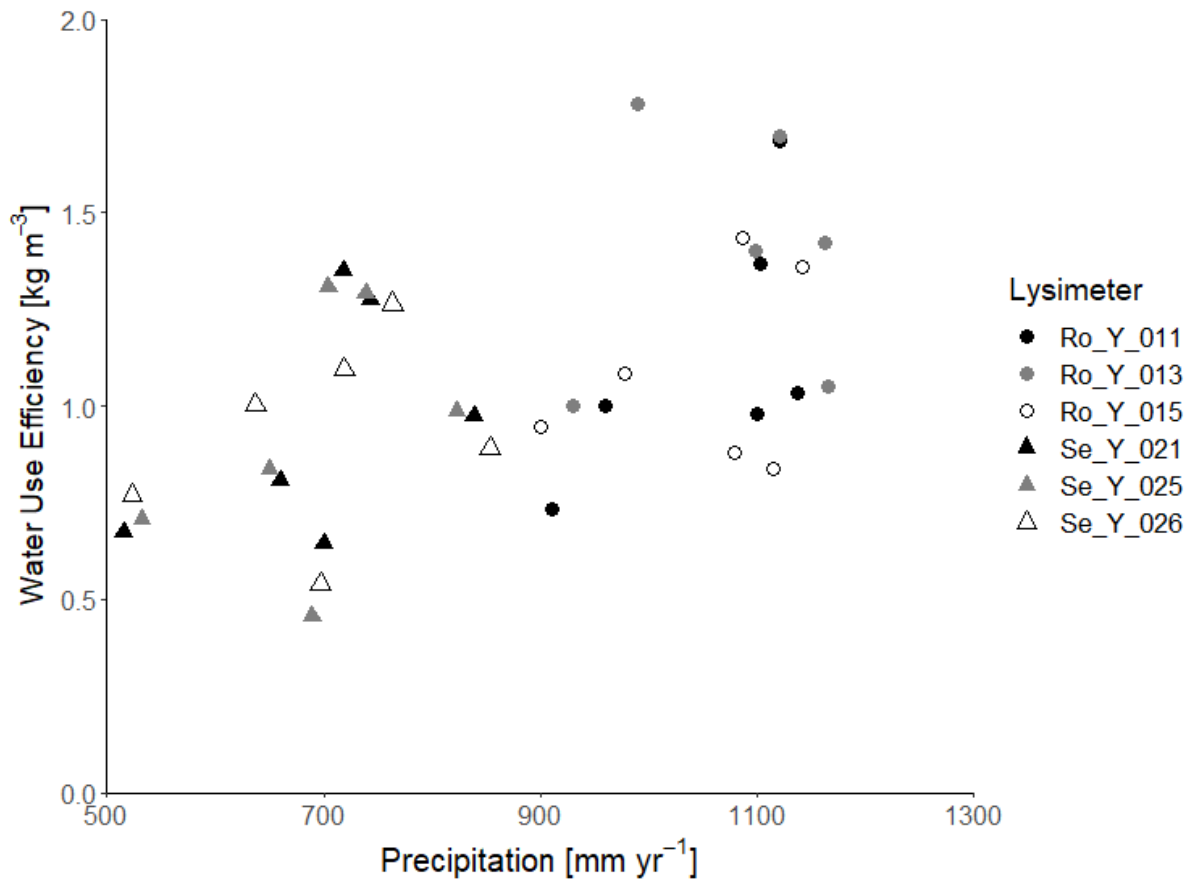


Figure 2. Water use efficiency (= annual harvest divided by annual evapotranspiration) as a function of annual precipitation at Selhausen and Rollesbroich.

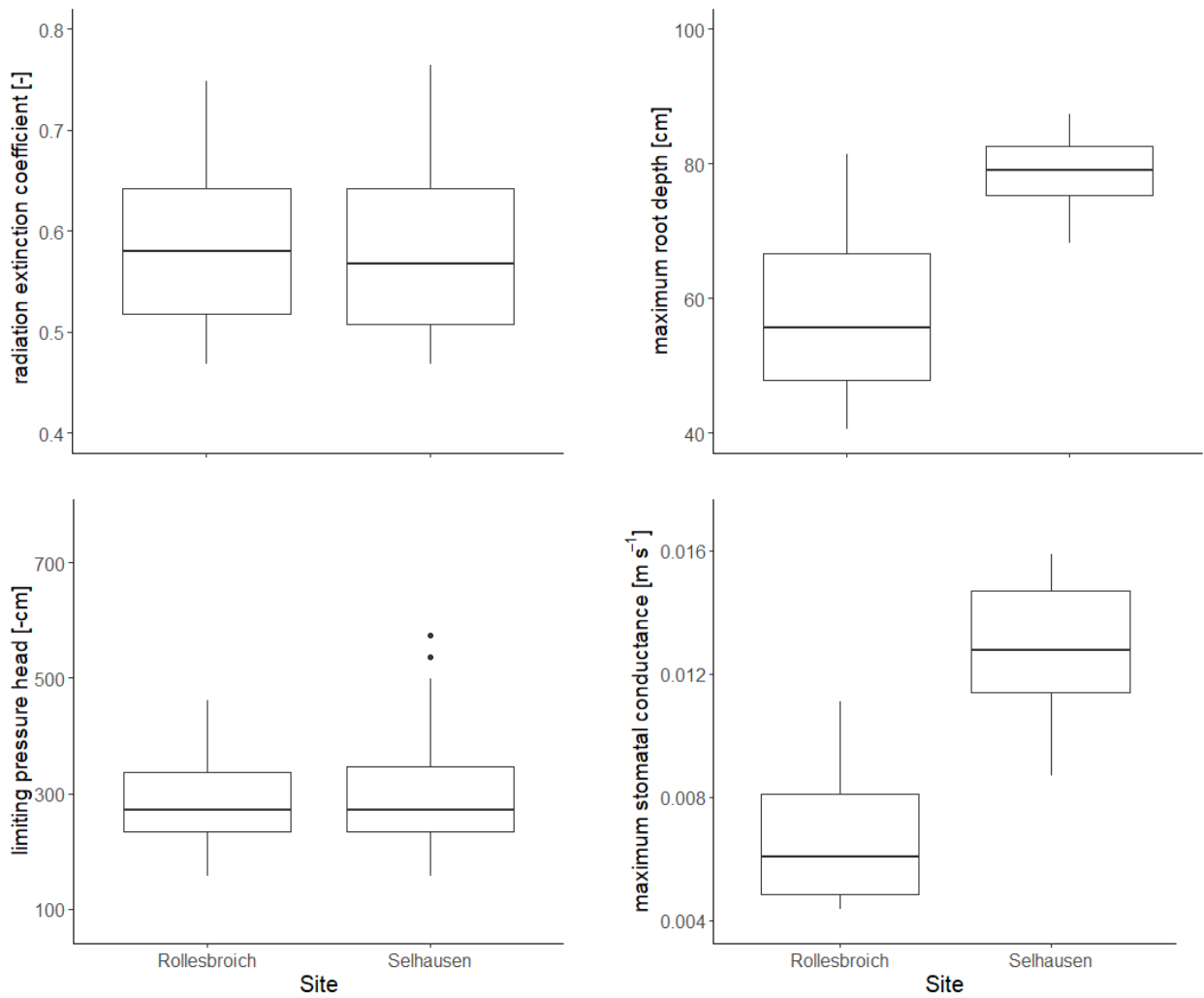


Figure 3. Posterior distributions of the four parameters treated as uncertain in the GLUE analysis. The horizontal line is the median value for the acceptable parameter sets, the box denotes 25th and 75th percentiles (inter-quartile range), the whiskers cover data points that lie within 1.5 times the inter-quartile range and solid circles represent outliers outside this range.

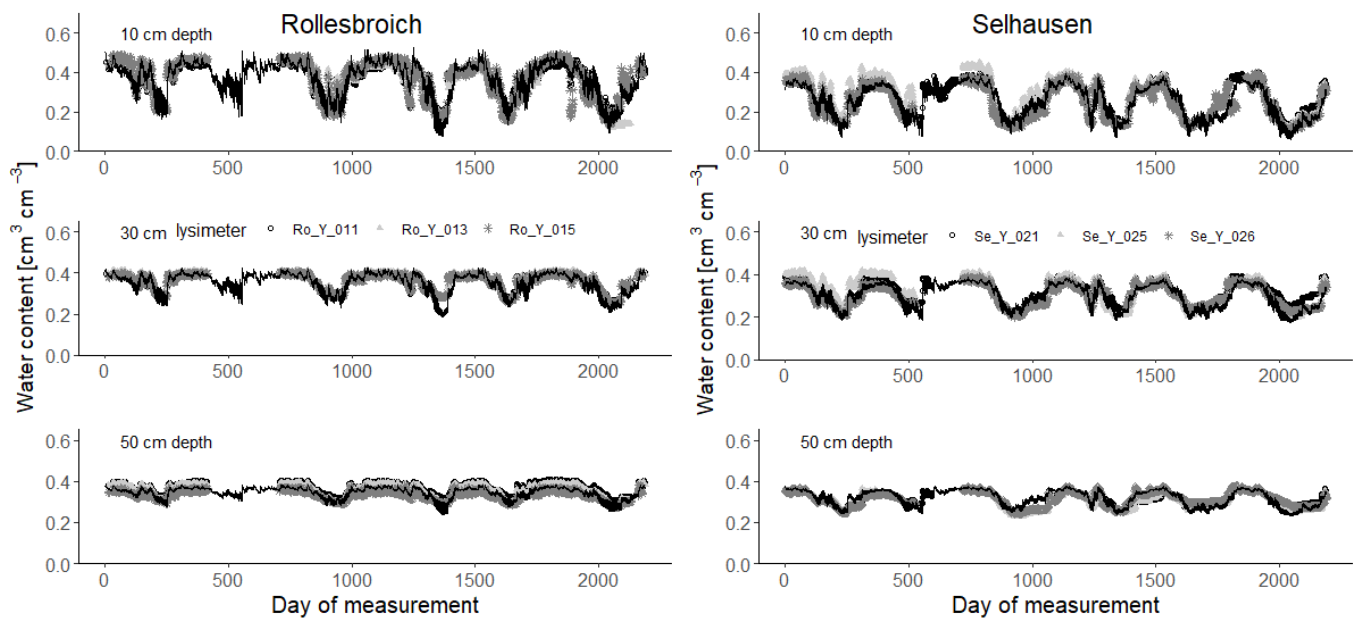


Figure 4. Measured soil water contents (symbols) at 10, 30 and 50 cm depth (2013-2018) compared with simulations for the 30 acceptable parameterizations at each site (black lines). Day 1 = 1st January 2013.

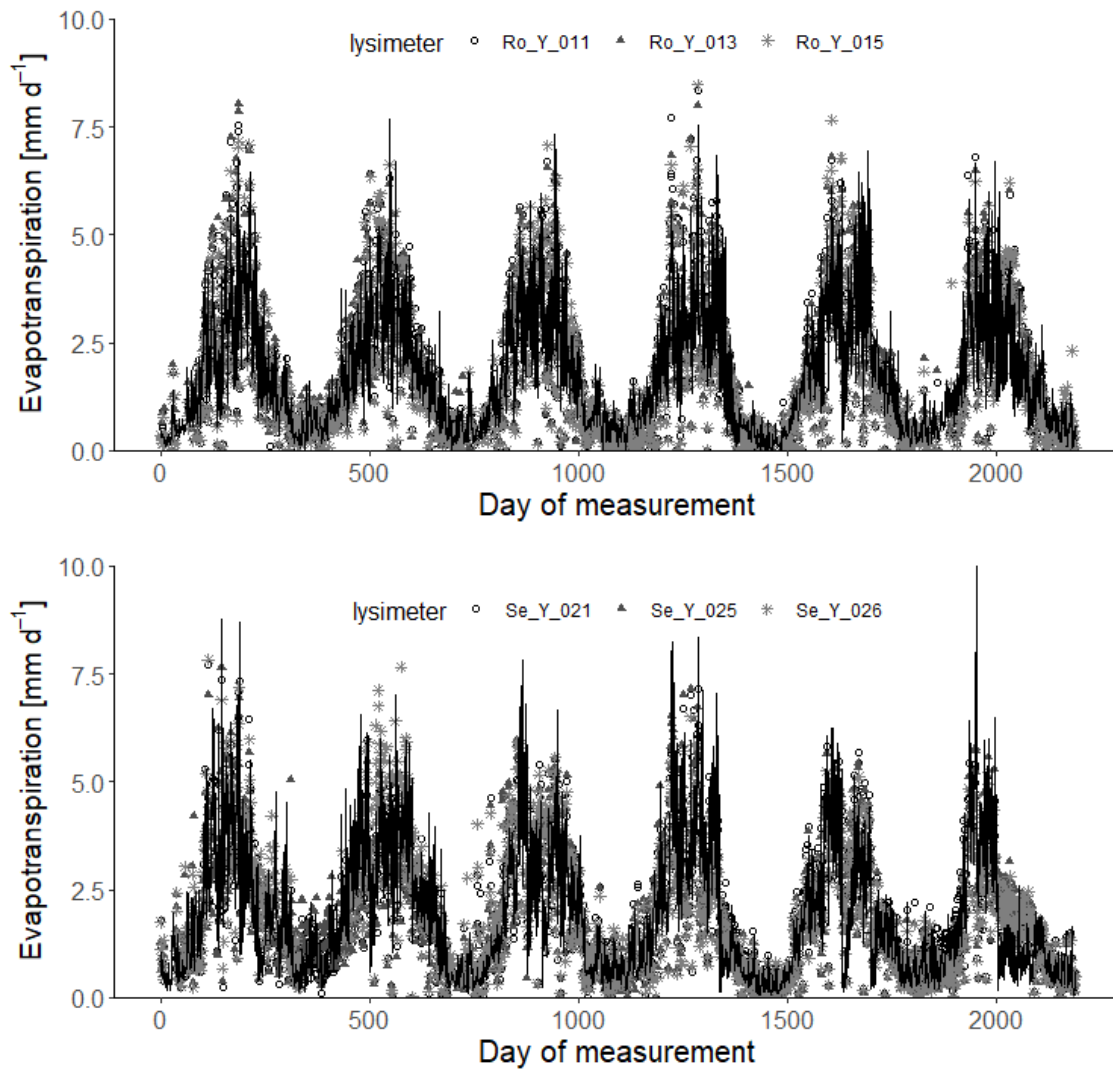


Figure 5. Measured daily evapotranspiration rates (symbols; 2013-2018) compared with simulations for the 30 acceptable parameterizations at each site (black lines). Day 1 = 1st January 2013.

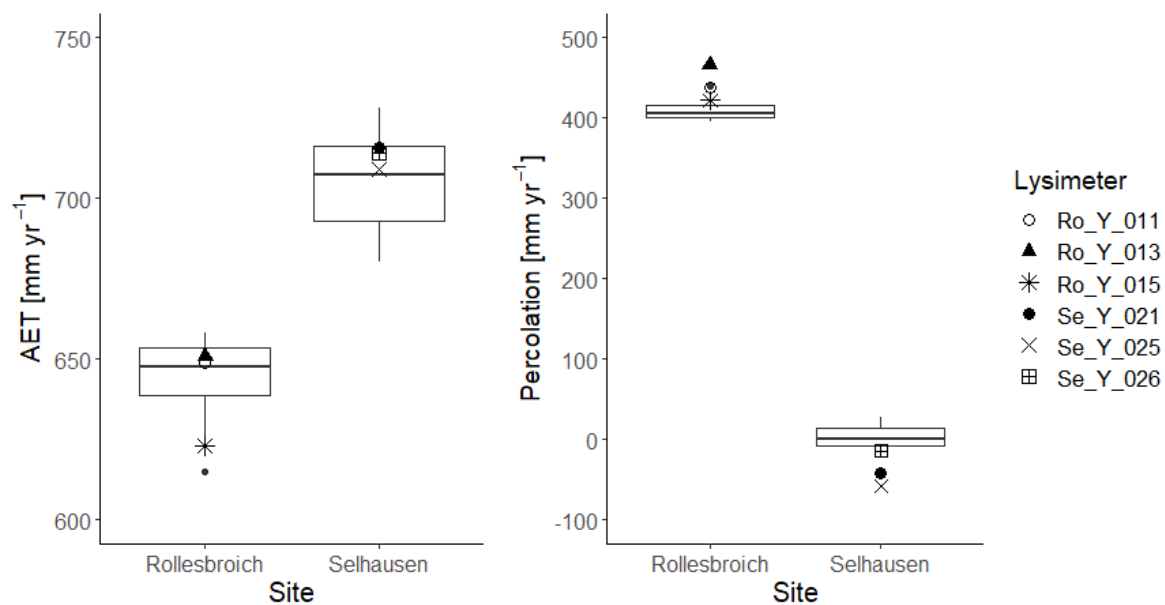
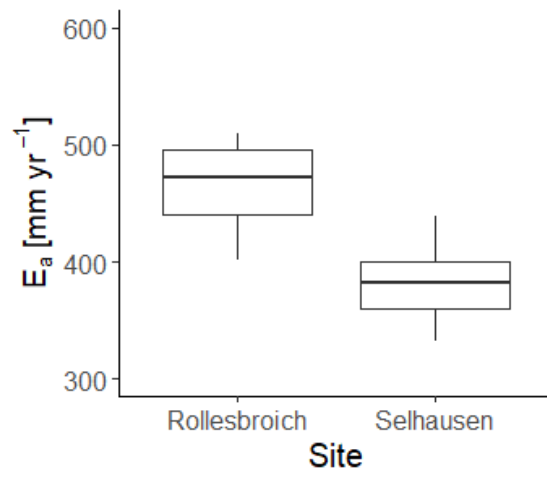
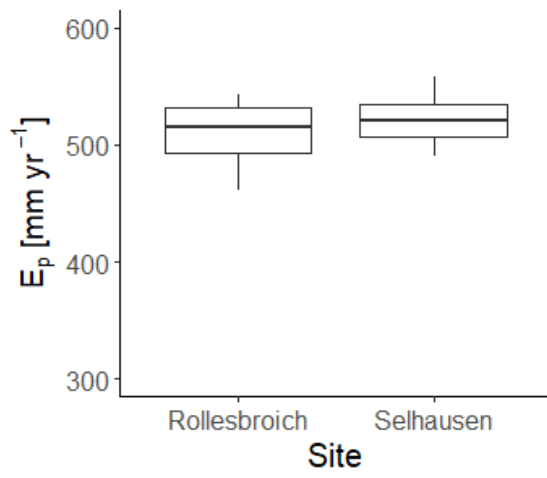
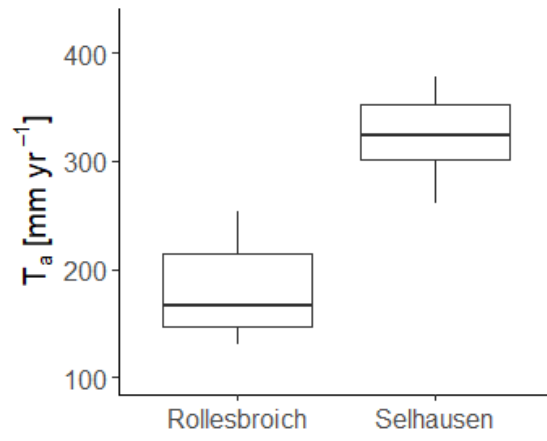
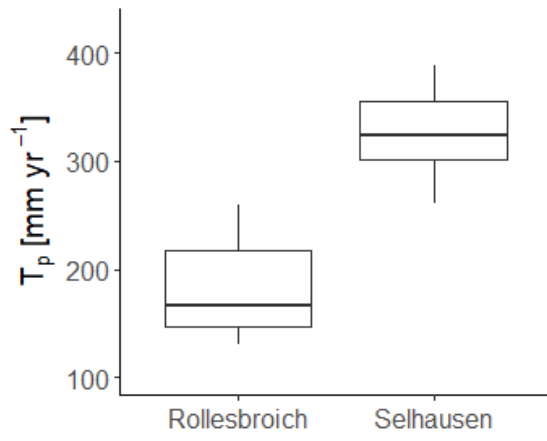


Figure 6. Box and whisker plots of simulated annual average evapotranspiration (AET) and percolation at Selhausen and Rollesbroich for the period 2013-2018 for the 30 acceptable simulations compared with the lysimeter measurements (large symbols). For an explanation of the box and whisker plots, see the caption to figure 3.



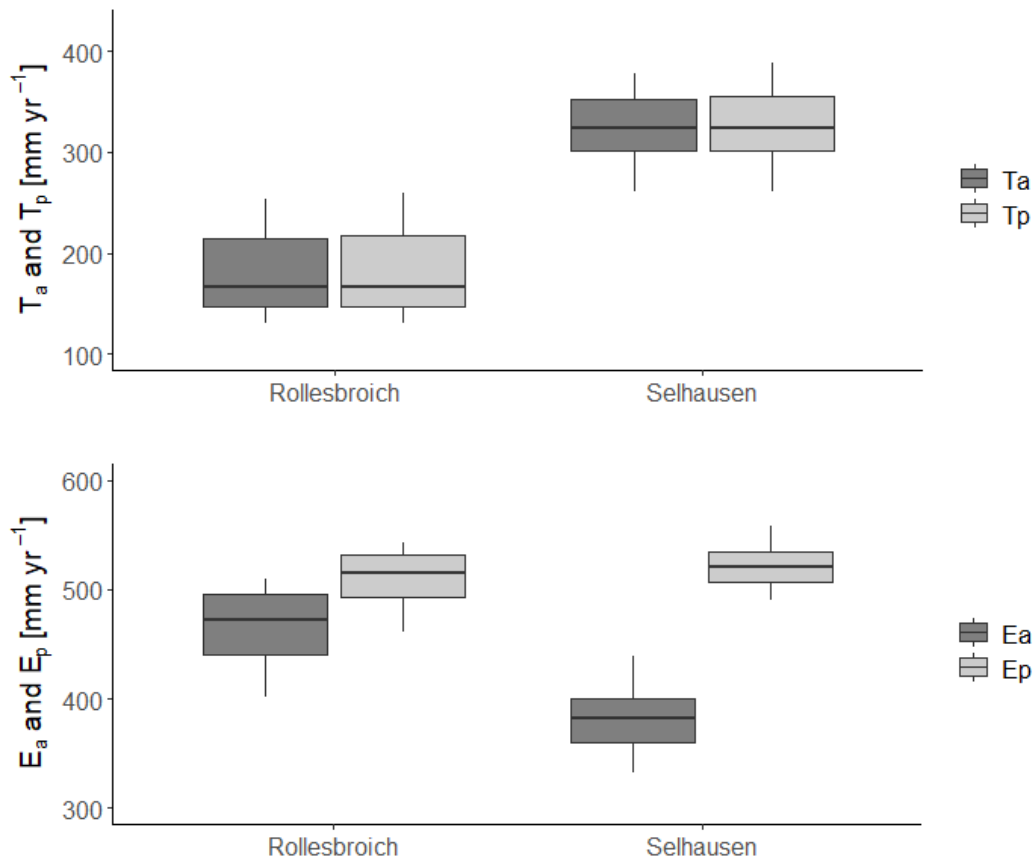


Figure 7. Simulated water balance terms for the 30 acceptable simulations at each site. For an explanation of the box and whisker plots, see the caption to figure 3.

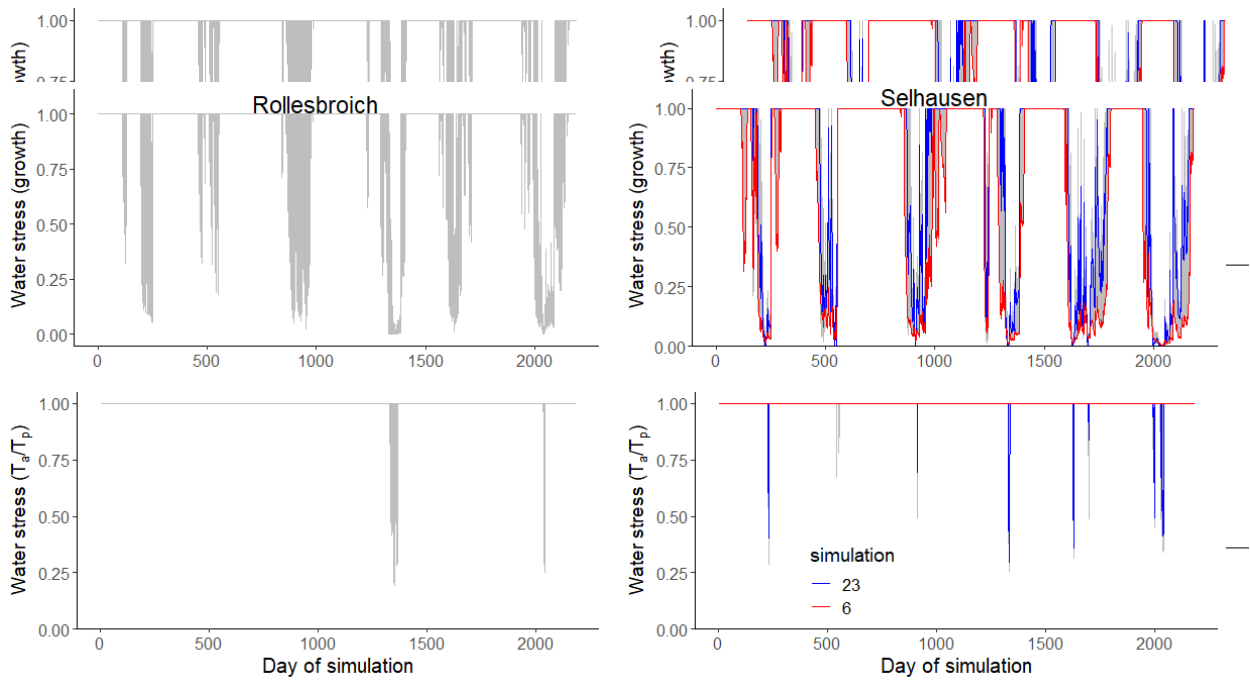


Figure 8. Plots of the two water stress functions in the model for the acceptable simulations. The uppermost figures show the threshold function of the pressure head at the root surface (equation 35) controlling dry matter allocation and leaf loss, while the figures at the bottom show the ratio of actual to potential transpiration, which controls assimilation (equation 34). Two contrasting acceptable simulations for the Selhausen site are highlighted in red and blue. [Day 1 = 1st January 2013.](#)

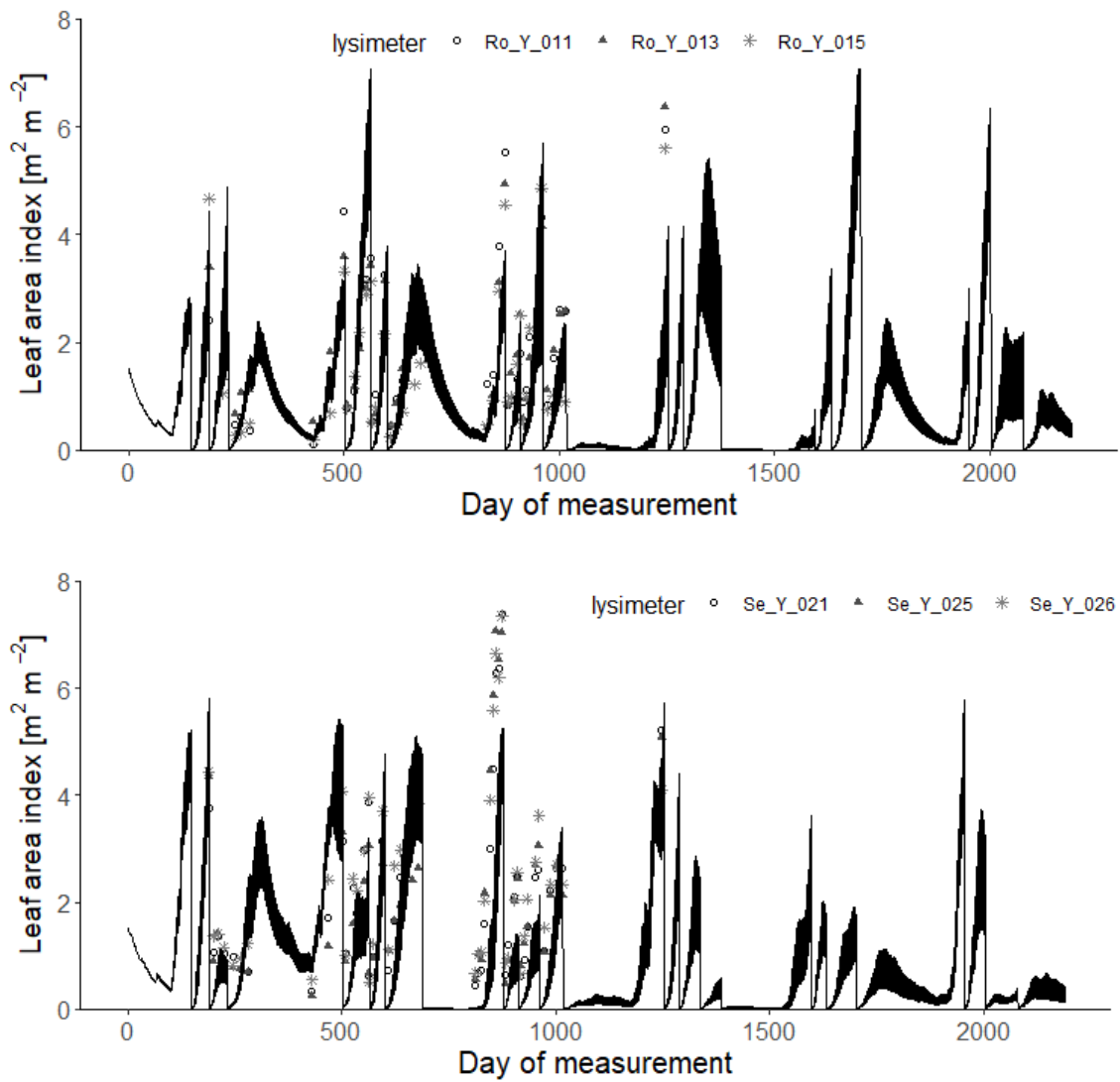


Figure 9. Measured daily leaf area index (symbols; 2013-2018) compared with simulations for the 30 acceptable parameterizations at each site (black lines). Day 1 = 1st January 2013.

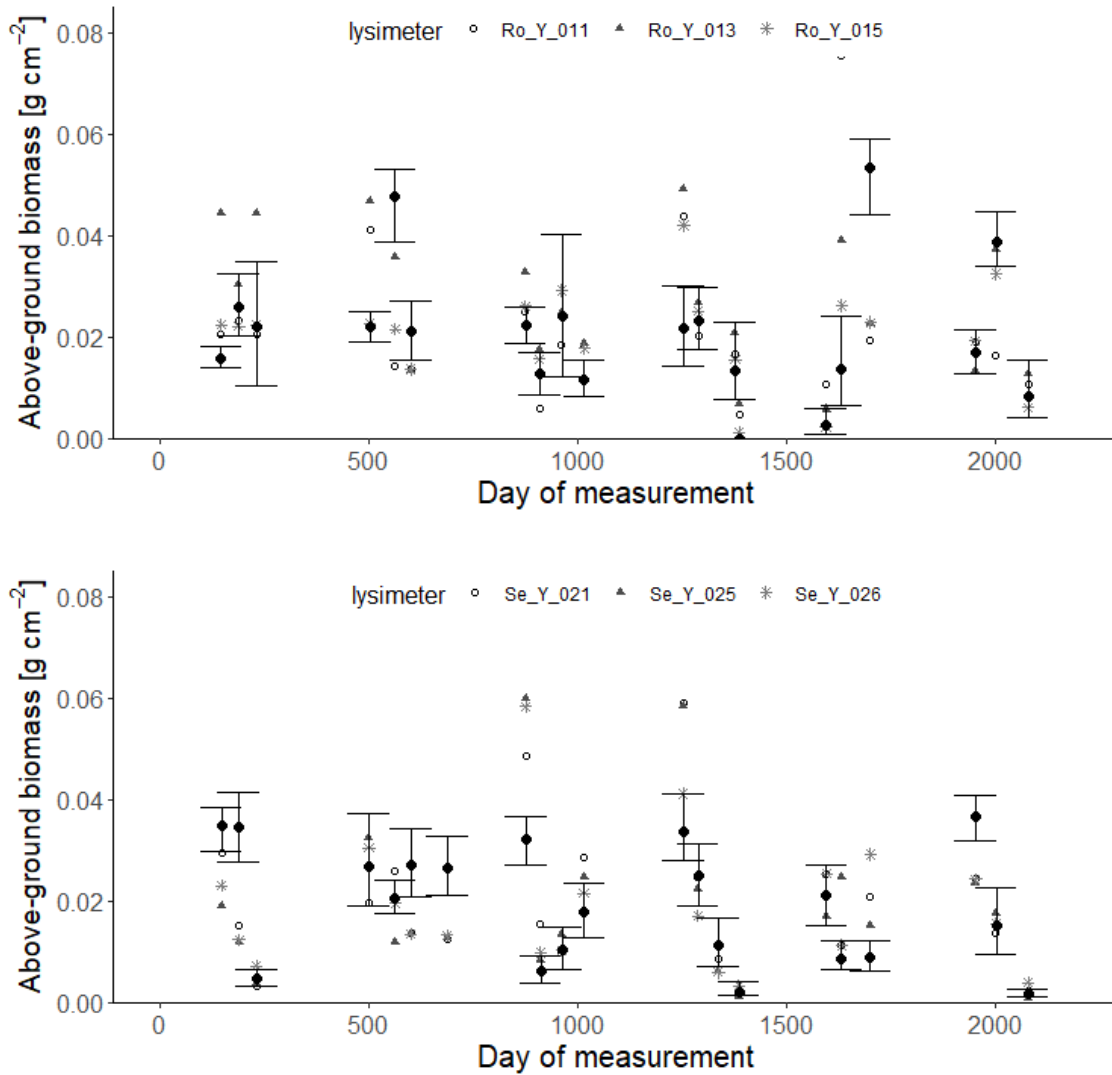


Figure 10. Measured harvests of above-ground biomass (symbols; 2013-2018) compared with simulations at each site (black symbols indicate means of the 30 acceptable parameterizations and the vertical lines denote minimum and maximum values). Day 1 = 1st January 2013.

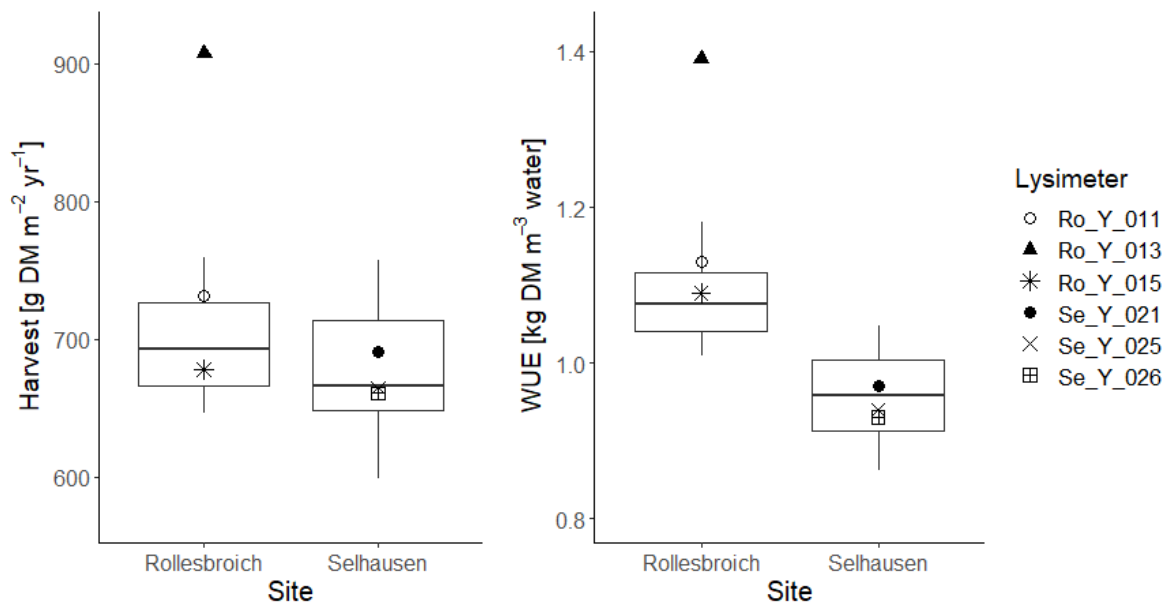


Figure 11. Box and whisker plots of simulated harvests and water use efficiencies (WUE, defined as total harvest divided by evapotranspiration) at Selhausen and Rollesbroich for the period 2013-2018 for the 30 acceptable simulations compared with lysimeter measurements (symbols). For an explanation of the box and whisker plots, see the caption to figure 3.

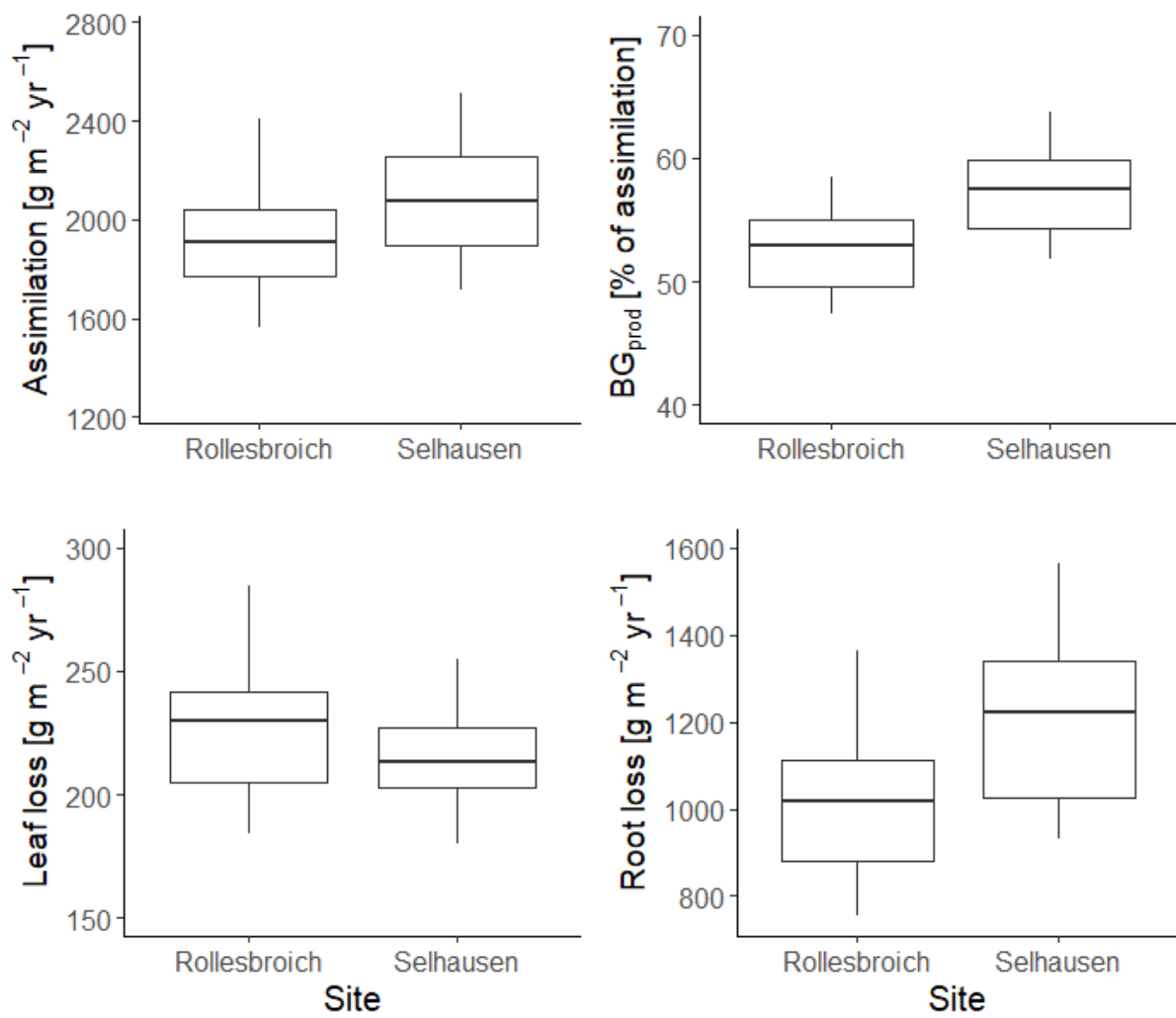


Figure 12. Box and whisker plots showing the simulated terms in the dry matter balance for the 30 acceptable model parameterizations at Selhausen and Rollesbroich for the period 2013-2018. For an explanation of the box and whisker plots, see the caption to figure 3.